

The Juno Mission

S.J. Bolton¹ · J. Lunine² · D. Stevenson³ · J.E.P. Connerney⁴ · S. Levin⁵ · T.C. Owen⁶ · F. Bagenal⁷ · D. Gautier⁸ · A.P. Ingersoll³ · G.S. Orton⁵ · T. Guillot⁹ · W. Hubbard¹⁰ · J. Bloxham¹¹ · A. Coradini¹² · S.K. Stephens⁵ · P. Mokashi¹ · R. Thorne¹³ · R. Thorpe¹

Received: 2 February 2015 / Accepted: 4 October 2017 / Published online: 2 November 2017
© Springer Science+Business Media B.V. 2017

Abstract Juno is a PI-led mission to Jupiter, the second mission in NASA's New Frontiers Program. The 3625-kg spacecraft spins at 2 rpm and is powered by three 9-meter-long solar arrays that provide ~500 watts in orbit about Jupiter. Juno carries eight science instruments that perform nine science investigations (radio science utilizes the communications antenna). Juno's science objectives target Jupiter's origin, interior, and atmosphere, and include an investigation of Jupiter's polar magnetosphere and luminous aurora.

Keywords Jupiter interior · Atmosphere · Magnetosphere · Juno

✉ S.J. Bolton
sbolton@swri.edu

¹ Southwest Research Institute, San Antonio TX, USA

² Cornell University, Ithaca NY, USA

³ California Institute of Technology, Pasadena CA, USA

⁴ NASA Goddard Space Flight Center, Greenbelt MD, USA

⁵ Jet Propulsion Laboratory, Pasadena CA, USA

⁶ Institute for Astronomy, University of Hawaii, Honolulu HI, USA

⁷ Laboratory for Atmospheric and Space Physics, University of Colorado, Boulder CO, USA

⁸ Observatoire Paris-Site de Meudon, Paris, France

⁹ CNRS, Université Côte d'Azur, Nice, France

¹⁰ Lunar and Planetary Laboratory, University of Arizona, Tucson AZ, USA

¹¹ Harvard University, Cambridge MA, USA

¹² Institute for Space Astrophysics and Planetology, Rome, Italy

¹³ University of California, Los Angeles CA, Italy

Acronym List (generally not including abbreviations or units)

APL	Applied Physics Laboratory
DSM	Deep Space Maneuver
DSN	Deep Space Network
EFB	Earth Flyby
EGA	Earth Gravity Assist
EOM	End of Mission
EOS	Equation of State
FDA	Fractional Data Allocation
GRAV	Gravity Science
GSFC	Goddard Space Flight Center
IOT	Instrument Operations Team
ITAR	International Traffic in Arms Regulation
JADE	Jovian Auroral Distributions Experiment
JEDI	Juno Energetic particle Detector Instrument
JIRAM	Jovian InfraRed Auroral Mapper
JOI	Jupiter Orbit Insertion
JPL	Jet Propulsion Laboratory
JSOC	Juno Science Operations Center
JunoCam	Juno Camera
KOZ	Keep Out Zone
MAG	Magnetometer
MHD	Magnetohydrodynamic
MOS	Mission Operations System
MPST	Mission Planning and Sequencing Team
MWR	MicroWave Radiometer
NAIF	Navigation and Information Facility
NASA	National Aeronautics and Space Administration
NAV	Navigation
PDS	Planetary Data System
PJ	Perijove
PRM	Period Reduction Maneuver
SAP	Science Activity Plan
SCT	Spacecraft Team
SPWG	Science Planning Working Group
SwRI	Southwest Research Institute
UCLA	University of California Los Angeles
UVS	UltraViolet Spectrograph

1 Introduction

Juno is the second mission in NASA's New Frontiers Program. The spacecraft was launched on 5th August 2011, made a flyby of Earth on 9th October 2013, and was inserted into orbit around Jupiter on 4th July 2016. Juno is a solar powered, spinning spacecraft during science operations (2 rpm), traversing much of the jovian magnetosphere in an elliptical polar orbit designed to minimize exposure to Jupiter's hazardous radiation environment.

Juno is a Principal-Investigator-led mission, developed in collaboration with the Jet Propulsion Laboratory as the management partner. The key institutions involved in Juno

Table 1 Institutional partners in Juno

Institution	Role on Juno
Southwest Research Institute	PI institution, two science instruments, science team
NASA Jet Propulsion Laboratory	Project management, mission management, Deep Space Network, two science instruments, science team membership, independent technical authority
Lockheed Martin	Spacecraft design and fabrication, integration and testing, mission operations
NASA Goddard Space Flight Center	Deputy PI institution, science instrument
IAPS/INAF Italy	Science instrument
U. Iowa, The Johns Hopkins University Applied Physics Laboratory, Malin Space Sciences Systems	Science instruments
California Institute of Technology, U. Michigan, Harvard U., U. Colorado, U. Leicester, U. Arizona, Cornell U., Georgia Institute of Technology, UCLA, Planetary Science Institute	Science team membership

Table 2 Key milestones during Juno development for flight and early mission activities

Date (UTC)	Event
1 Jun. 2005	Selection for flight (Phase B)
1 Sep. 2008	Phase C
1 Apr. 2010	Phase D
5–26 Aug. 2011	Launch period; launch occurred on 05 August 2011
9 Oct. 2013	Earth flyby
5 Jul. 2016	Jupiter Orbit Insertion
30 Jul. 2021	Planned completion of primary mission

are listed in Table 1. Juno was proposed in response to the 2003 Announcement of Opportunity for New Frontiers missions. Juno was selected to carry out a competitive Phase A study in 2004, and was selected for development for flight (start of Phase B) in 2005. The key milestones during the subsequent development for flight are listed in Table 2. The Juno mission was reviewed by Grammier (2009), Nybakken (2011, 2012), Bernard et al. (2013), Lewis (2014), and Stephens (2015).

The Juno baseline science objectives are satisfied with 32 orbits, a spin-stabilized solar powered spacecraft, radiation shielding, and a unique payload including microwave receivers, X- and Ka-band radio science hardware, vector magnetometers, high- and low-energy charged particle detectors, radio and plasma wave antennas, UV and IR spectroscopic imagers, and a visible light public outreach camera (see Fig. 1a). Science observations are made in a limited number of orientations, primarily one for gravity science (spin axis and main antenna pointing to Earth), and one for microwave atmospheric sounding (spin axis perpendicular to orbit plane to allow nadir pointing in the spin plane). Prime science data are collected near closest approach (perijove), along with calibrations, occasional remote sensing, and continued magnetospheric observations in the outer parts of the orbits.

Juno's highly elliptical, polar trajectory avoids Jupiter's highest radiation regions and provides a series of passes close to the planet (Fig. 1b), allowing close-in observations of Jupiter's interior, deep atmosphere, high order magnetic field and polar magnetosphere. Juno

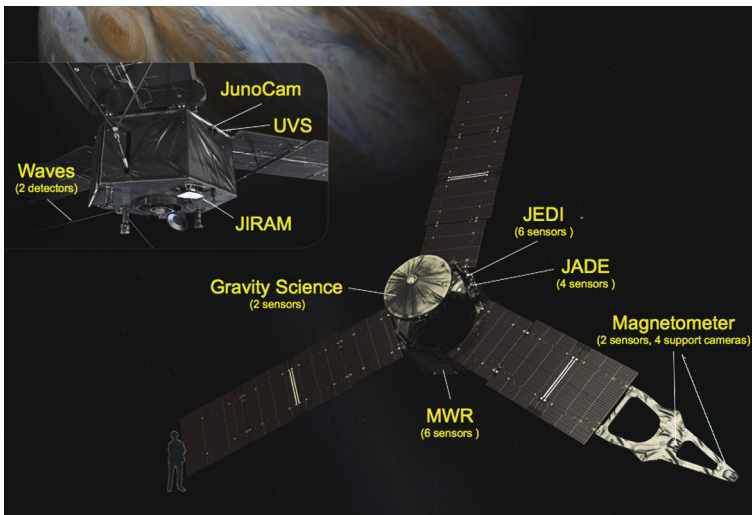


Fig. 1a NASA's Juno spacecraft and science payload

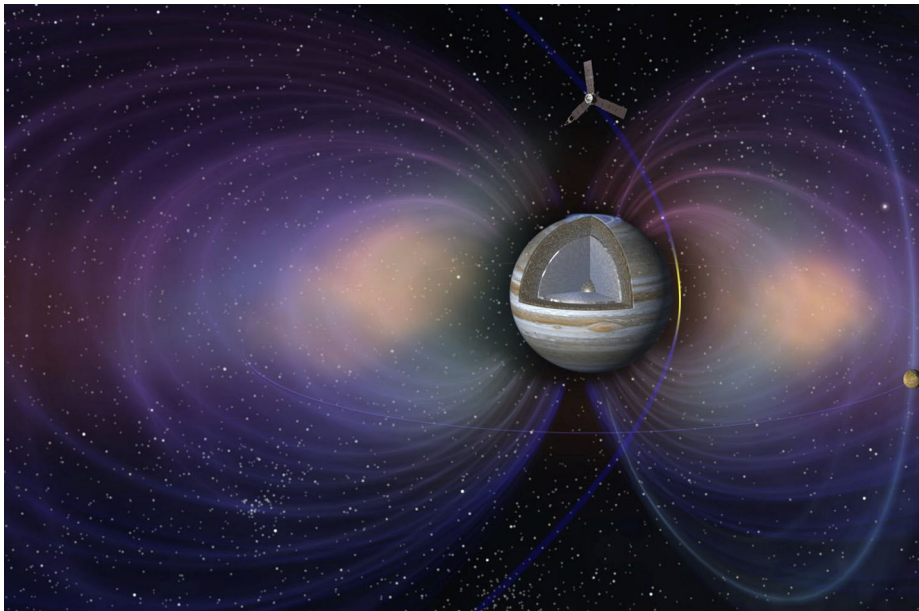


Fig. 1b NASA's Juno spacecraft takes an orbit over Jupiter's poles, ducking under the radiation belts, and skimming over the clouds. Carrying nine scientific instruments on a spinning spacecraft, the Juno mission addresses key issues about the magnetosphere, atmosphere, and deep interior of the giant planet

spends a few hours very close to the planet approximately every 53 days, reaching an apo-
jove distance of nearly 8 million km (113 jovian radii where an R_J is 71,492 km) before
returning. The result is a series of close flybys, minimizing exposure to damaging radiation
from Jupiter's radiation belts while enabling measurements in close proximity to Jupiter.

Taking advantage of Jupiter's 10-hour rotation, the orbital period is slightly adjusted for each pass to observe a specific longitude, ultimately providing a magnetic map with complete longitudinal coverage. The low-perijove altitude provides close-in magnetic and gravitational measurements, as well as observations from the 6-channel MicroWave Radiometer (MWR), which passively measures Jupiter's thermal emission from beneath the synchrotron-emitting radiation belts.

In Sect. 1 of this paper, we present a brief overview of the Juno mission, the spacecraft, science instruments, and spacecraft trajectory. In Sect. 2 we discuss Juno's science objectives related to Jupiter's formation, interior structure, and dynamical evolution (atmosphere and magnetosphere). In Sect. 3 we show how Juno is operated via the Juno Science Operation Center. Further discussion on the mission science can be found in the instrument chapters.

1.1 Scientific Objectives

Solar system formation models all begin with the collapse of a portion of a molecular cloud to form a protoplanetary disk, conventionally called for our planetary system the solar nebula during the time period it is dominated by gas. Jupiter, at a distance of 5.2 AU, is the most massive planet in our solar system, with a mass of ~ 318 Earth masses (M_{\oplus}). Jupiter consists mostly of hydrogen and helium, with traces of heavier elements. Because Jupiter was formed primarily of gaseous H and He, it must have formed early, while the solar nebula was still present. How this happened, however, is unclear. Two endmember mechanisms are (i) direct instability of the disk itself and (ii) accretion of a solid core inducing local collapse of gas around it. Differences between these scenarios are profound. More importantly, the composition and role of planetesimals in planetary formation remains poorly understood—and as a result, the origin of Earth and other terrestrial planets also remain poorly understood. The role of icy planetesimals—the carriers of volatile species, including water and organics that are the fundamental building blocks of life and produced bio-molecules on early Earth—is particularly noteworthy.

Juno measures the deep-water abundance within Jupiter and determines whether the solar system's largest planet has a core of heavy elements (those other than hydrogen and helium), directly addressing the planet's origin and thereby that of the solar system. By mapping its gravitational and magnetic fields, Juno reveals Jupiter's interior structure and constrains the mass of its core. How deep Jupiter's zones, belts, and other features penetrate is a fundamental question in jovian atmospheric dynamics. By mapping variations in atmospheric composition, temperature, cloud opacity and dynamics to depths much greater than 100 bars at all latitudes, Juno determines the global structure and dynamics of Jupiter's atmosphere below the cloud tops for the first time. Jupiter's powerful magnetospheric dynamics create the brightest aurora in our solar system, as electrons and ions precipitate down into its atmosphere. Before Juno, observations of Jupiter's aurora were limited to remote imaging. Juno directly measures the distributions of these charged particles, their associated fields, and the concurrent UV and IR emissions of Jupiter's polar magnetosphere. This greatly improves our understanding of one of the most remarkable phenomena of our solar system.

1.2 Spacecraft, Instrumentation, and Orbit Geometry

1.2.1 Juno Spacecraft

Juno is the first solar-powered mission to Jupiter. The spacecraft carries three arrays with 11 solar panels where the length of each solar arm is 29.5 feet (9 meters) and the width is 8.7

feet (2.65 meters). This makes a total surface area more than 650-foot (60-meters) squared, covered with 18,698 individual solar cells. Total power output at Earth's distance from the sun is approximately 14 kilowatts. At Jupiter, the total power output is approximately 500 watts. The total mass of Juno was 7,992 pounds (3,625 kilograms) at launch, consisting of 3,513 pounds (1,593 kilograms) of spacecraft, plus 2,821 pounds (1,280 kilograms) of fuel and 1,658 pounds (752 kilograms) of oxidizer. The science instruments are distributed on the forward and aft decks, except for the magnetometers, located at the end of one of Juno's solar arrays. The spacecraft electronics are located in a titanium enclosure that acts as a radiation shield, located on the forward deck. The radiation shield—a hollow cube about 1 m on a side—also structurally supports the 2.5-meter X/Ka high gain antenna.

The cumulative radiation dose (Total Ionizing Dose, or “TID”) to be experienced by Juno from launch to the end of the science mission is much higher than that experienced on previous missions. The total ionizing dose for the Juno mission is equivalent to about ~100 krad Si, behind ~1/2 inch equivalent of aluminum shielding. The estimated Juno TID is greater than a factor of 10 that of contemporary missions (Cassini and MRO), and a factor of four greater than the Galileo mission. The design of the spacecraft to handle such high radiation as well as plans for implementing the mission are discussed by Kayali et al. (2012) and Guertin et al. (2012). The radiation experienced by Juno is monitored throughout the mission via noise signatures of penetrating radiation measured within science and engineering instruments (Becker et al. 2017, this issue).

1.2.2 Science Instruments

The Juno spacecraft carries instruments for nine science investigations, as listed in Table 3. The spacecraft rotates twice per minute about a spin axis that is nearly perpendicular to the orbital plane, and all the remote sensing instruments look outward in the spin plane, so that each instrument has multiple opportunities to look both towards Jupiter and towards the radiation belts, rings, and deep space. As the trajectory evolves over the mission, the solar panels (and spin axis) are kept pointed towards the Sun for most of the orbit with some tilting of the spin axis for specific passes to enhance observations of Jupiter.

The interior of Jupiter is explored via measurement of the gravity field (Asmar et al. 2017, this issue) and magnetic field (Connerney et al. 2017, this issue). The atmosphere of Jupiter is explored via conventional visible imaging (Hansen et al. 2017, this issue) and infrared spectroscopy and imaging (Adriani et al. 2017, this issue), but also via a new technique of microwave sounding (Janssen et al. 2017, this issue) that measures emissions in six wavelength bands between 1.3 and 50 cm. The structure and dynamics of the upper atmosphere and aurora are explored via their UV (Gladstone et al. 2014, this issue) and IR (Adriani et al. 2017, this issue) emissions. Magnetospheric particles (ions and electrons) are measured by the JADE (McComas et al. 2013, this issue) and JEDI (Mauk et al. 2013, this issue) instruments which span nearly six orders of magnitude in energy. Juno's magnetometer (Connerney et al. 2017, this issue) measures the magnetospheric magnetic structure while the Waves instrument (Kurth et al. 2017, this issue) measures radio and plasma waves (electric and magnetic fields).

1.2.3 Juno's Trajectory

Juno was launched on 5 August 2011 and reached Jupiter using a “delta-vega Earth Gravity Assist” (Δ V-EGA) trajectory (Fig. 2), with large Deep Space Maneuvers (DSMs) 13 months

Table 3 Science packages and instruments on Juno

Instrument	Institution	Description	Science investigation
Gravity Science (GRAV)	JPL	X- & Ka-band uplink and downlink	Interior structure
Magnetometer (MAG)	GSFC	2 Vector fluxgates (FGM) & 4 co-located star cameras	Interior structure & magnetic dynamo
MicroWave Radiometer (MWR)	JPL	6 wavelengths (1.3–50 cm)	Deep atmosphere sounding & composition
Juno Energetic particle Detector Instrument (JEDI)	APL	Ions 0.015–20 MeV Electrons 0.02–1 MeV	Auroral particle distributions, ion composition
Jovian Auroral Distributions Experiment (JADE)	SwRI	Electrons 100 eV–100 keV Ions 10 eV–40 keV	Auroral particle distributions, ion composition
Waves	U. Iowa	4 m electric dipole & magnetic search coil E-field 50 Hz–40 MHz B-field 50 Hz–20 kHz E bursts 50 Hz–100 kHz B bursts 50–20 kHz Waveforms 1.0 MHz bandwidth	Radio & plasma waves
UltraViolet Spectrograph (UVS)	SwRI	FUV spectral imager wavelength 70–205 nm with 125 km resolution	Spatial & temporal auroral structure
Jovian InfraRed Auroral Mapper (JIRAM)	IAPS/INAF, Italy	IR spectral imager 2–5 microns	Spatial & temporal atmospheric structure and dynamics
JunoCam Juno Camera	Malin Space Sciences Systems	Visible imager	Atmospheric dynamics and structure

after launch and an Earth Flyby (EFB) 26 months after launch. Transit time to Jupiter after Earth Flyby was another 33 months.

The 53-day capture orbit was designed to save fuel compared to direct insertion into the originally-planned 11-day (and subsequently, 14-day) orbits, via (a) minimizing DSM ΔV by arriving at Jupiter earlier, and (b) lowering gravity losses. Jupiter Orbit Insertion (JOI) on 7/5/16 UTC (7/4/16 in the United States) was timed so that two capture orbit periods resulted in a 10/19/16 date for the Period Reduction Maneuver (PRM) which was planned to occur two perijoves (PJ) later. The PRM would have put the spacecraft into a 14-day period, but due to concerns about the reliable operation of check valves in the propulsion system, the PRM was canceled and the decision was made to remain in 53-day orbits.

The Juno polar, highly elliptical orbit is designed to facilitate close-in measurements of Jupiter while avoiding the regions of most severe radiation. Each perijove slides between Jupiter's main radiation belts and the upper atmosphere at an altitude below 8000 km. Figures 3a, 3b, 3c, 3d illustrate several views of Juno's 35 orbits (including 32 baseline science orbits and 1 spare) around Jupiter. A deorbit maneuver near apojoive of the final orbit puts the Juno spacecraft into Jupiter, to comply with planetary protection for the Galilean moons.

Although called a 53-day orbit, it is actually 53 days times 0.9975 or 52.867 days on average. The difference arises from the time between solar conjunctions ($0.9975 = 1 - 1/399$, where 399 days is the synodic period of Jupiter with respect to the Earth). This maintains

Fig. 2 View of Juno’s trajectory from launch to Jupiter Orbit Insertion (JOI). The trajectory included an Earth flyby (EFB) and two Deep Space Maneuvers (DSMs)

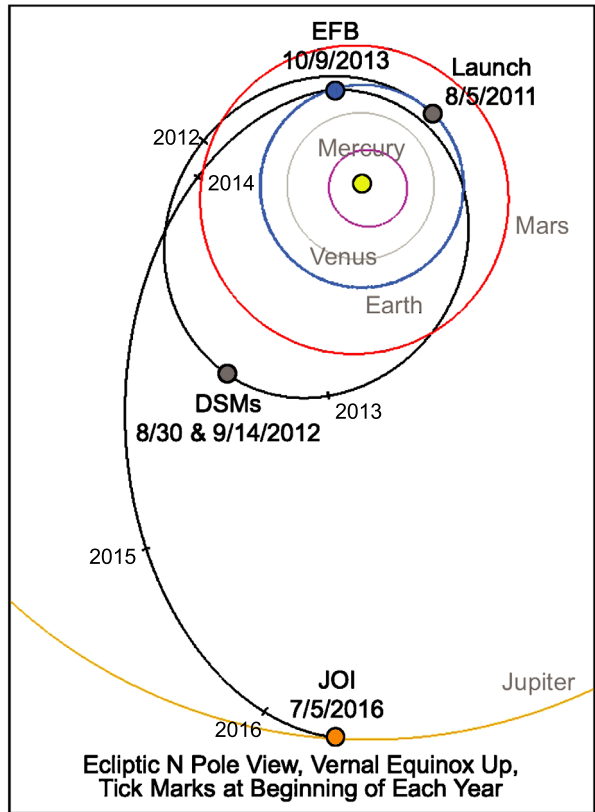
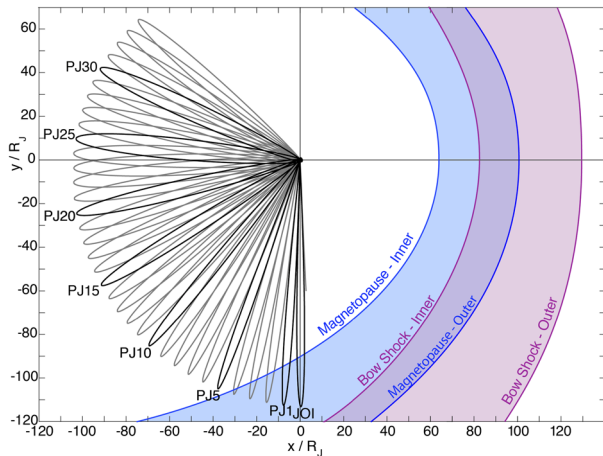


Fig. 3a Juno’s 53-day orbit viewed in the jovian equatorial system where the x -axis points towards the Sun, and the z -axis is Jupiter’s spin axis. Projection of Juno’s trajectory into the equatorial ($x-y$) plane



perijoves over one DSN station, DSS-25 at Goldstone, which currently is the only station with Ka-band uplink capability.

The 35-orbit duration of the prime mission takes 5.07 years, during which Jupiter moves nearly half way around the Sun. As a result, the orbit moves from dawn around to the night

Fig. 3b View from the Sun showing the projection of Juno’s trajectory in the y - z plane

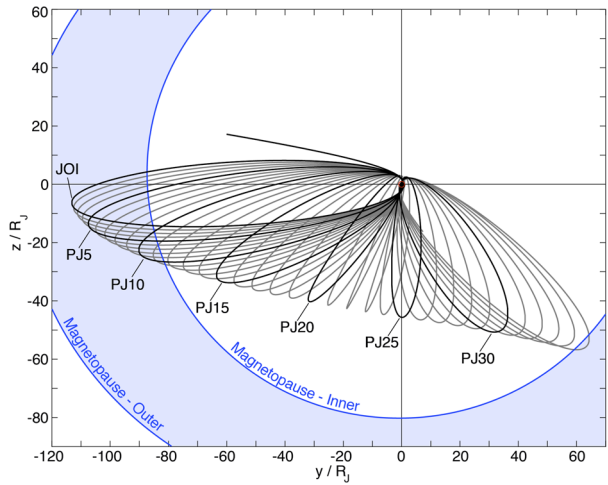
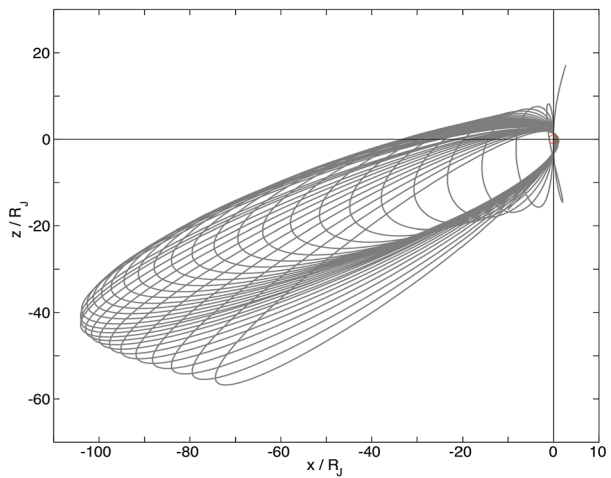


Fig. 3c Projection of Juno’s trajectory in the x - z plane



side of Jupiter and into the mid-evening sector (Fig. 3a). The oblateness of Jupiter causes the orbit to precess southward at about 1° per orbit. The southward precession of the orbit means that the equator-crossing on the inbound leg of the orbit moves inwards from $104 R_J$ to $13 R_J$ by orbit 34 (Fig. 3d). Juno was conceived as a polar orbiter with inclination near 90° , but to avoid an eclipse after PJ22 in 53-day orbits, the inclination will be allowed to grow as large as 105.5° (with a concurrent change in the ascending node of the orbit). The apsidal rotation is shown in Figs. 3c and 3d. A large orbit trim maneuver is performed near the apojoove between PJ22 and PJ23 to contribute to the inclination change in order to avoid the spacecraft going through an eclipse.

A key aspect of Juno’s investigation is the mapping of Jupiter provided by 32 successive close polar passes, each at a specific longitude, resulting in a complete high-resolution map of the entire planet for both the magnetic and gravity field investigations as seen in Fig. 4. Orbit trim maneuvers shortly after perijove are used to target the timing of subsequent perijoves so that the longitudes of post-perijove equator crossings are evenly spaced, 11.25° apart, after 32 science orbits. They build up in a 4-8-16-32 pattern, with evenly spaced lon-

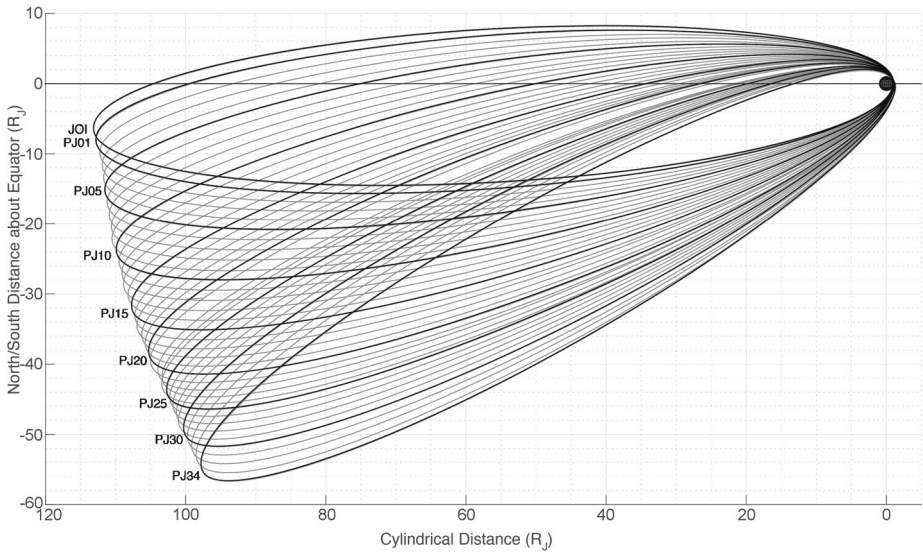


Fig. 3d View of Juno's trajectory perpendicular to the orbit plane. There were no science data during Jupiter Orbit Insertion (PJ0) and PJ2

gitudes 90° apart after 4 orbits, 45° apart after 8 orbits, 22.5° apart after 16 orbits, and 11.25° apart after 32 orbits, lending robustness to the magnetic field investigation in case of missed longitudes or premature mission termination. With JOI counting as perijove 0 (PJ0), the first orbit with a longitude useful for the magnetic field investigation was PJ1. No useful science was achieved at PJ2 (aside from X-band tracking for gravity science) due to the decision to cancel the PRM, and the subsequent pre-PJ2 safe mode entry. PJ3 through PJ33, if all are successful, will finish the 32 baseline science orbits along with PJ1. PJ34 is the spare perijove, and PJ35 on 7/30/21 marks the planned End of Mission (EOM) with an impact into Jupiter after the deorbit maneuver.

For a planned 5-year Jupiter mission, with 36 total perijoves of 53-day orbits, the minimum and maximum Earth ranges (opposition and solar conjunction) each occur roughly every 13 months. Sun range reached a maximum of 5.46 AU in early 2017 (Jupiter aphelion), and will decrease to 5.03 AU at EOM in mid-2021. The one-way Earth-Juno light travel time varies between about 34 and 53.5 minutes.

Gravity science requires communicating with the DSN (Earth-pointed spin axis), and microwave atmospheric sounding requires nadir pointing (spin axis perpendicular to orbit plane). These two primary spacecraft spin-axis orientations (Gravity Science = GRAV, and MicroWave Radiometer = MWR) support most mission science measurements. MWR attitudes are used in early orbits when the resulting spin-axis to Sun angle is not too large and the solar arrays can supply sufficient power. Earth-pointed GRAV attitudes are used in most of the other orbits, so that two-way X- and Ka-band links between the DSN and the HGA are maintained for the perijove pass. After about PJ9, MWR and other attitudes under consideration with a significant off-Sun angle for the solar arrays can only be maintained for very limited durations near perijove.

GRAV favors the geometry near opposition, since small Sun-Earth-Juno angles near conjunction increase noise from the Sun's corona for X-band, which is more susceptible than Ka-band. MWR attitudes may also be usable if an extended mission is performed, when the

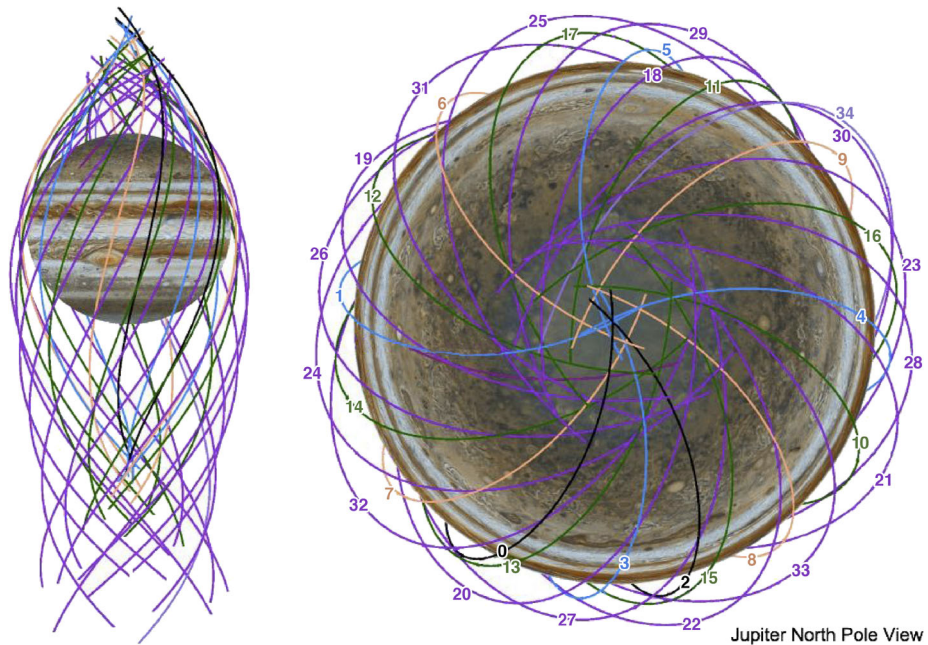


Fig. 4 Juno passes north to south in about two hours. There were no science data during Jupiter Orbit Insertion (PJ0) and PJ2 (*black*). The orbits are spaced in longitude to allow mapping of the planet at increasing resolution (90° *blue*, 45° *orange*, 22.5° *green* and 11.25° *purple*)

off-Sun angle is again more favorable. Radiation accumulation occurs mainly during the part of the orbit coming in to perijove, and increases substantially as the orbital line of apsides (connecting perijove and apojove) rotates due to Jupiter's oblateness, and as perijove latitude increases from 3° at JOI to 31° at PJ35. Radiation is expected to be the main limitation to Juno's mission lifetime.

Juno utilizes JSOC, the Juno Science Operations Center, for ground data and mission operations systems and to facilitate the distribution and archiving of data (see Sect. 3 below).

2 Juno Science Goals and Objectives

2.1 Formation of the Giant Planets

Giant planets are the alpha and omega of planetary formation and evolution. They are the beginning because they are rich in the primary cosmic elements hydrogen and helium, and must form within the first few million years when the protoplanetary disk is in its gaseous, solar nebula stage. Because of their large gravitational fields, Jupiter and Saturn then played primary roles in the scattering of solid material, dynamically exciting the solids and ejecting a large fraction from the solar system. They therefore accelerated terrestrial planet growth and brought it to a quick end after roughly 10^8 years (Chambers and Wetherill 1998).

Juno will provide information on Jupiter's formation via three key measurements. First, the measurements of Jupiter's global water abundance from microwave radiometry up to pressures of 100 bars will provide constraints on the water total abundance (Janssen et al.

2017, this issue). Second, the measurements of high-order gravitational coefficients will provide constraints on the distribution of mass within Jupiter, and the possibility of a central core of heavy elements (Asmar et al. 2017, this issue) and finally, measurements of Jupiter's magnetic field may also provide information on the state of the interior (transition from molecular to metallic hydrogen) and possibly differential rotation when related to dynamo theories (Connerney et al. 2017, this issue). A determination of the core mass is important because a very large ($> 10 M_{\oplus}$) or very small (i.e., undetected) core will set constraints on the sequence of accretion of solids and gas, and possibly on the size of the solid bodies that were swept up by Jupiter.

Jupiter likely grew more rapidly than any other planet, being much more massive than the other planets. One class of models proposes that a proto-planetary core (~ 10 or more Earth masses) was formed by accretion of solids, followed by collapse of the surrounding hydrogen and helium (Mizuno 1980; Lissauer 1993; Pollack et al. 1996a,b; Wuchterl et al. 2000; Hersant et al. 2001). This class of models yields a planet with a central dense core of at least 10 Earth masses (M_{\oplus}) beneath a hydrogen–helium envelope. However, the central heavy element core need not be fully discrete (Lozovsky et al. 2017); it may be somewhat diffuse. In these core accretion models, the timescale for the accretion of gas is relatively long, with a duration of up to several million years for the mass of accreted gas to become comparable to the core mass. It is much shorter, of order 10^4 years, for accretion of most (the final $\sim 90\%$) of the remaining mass. An alternate model proposes a much faster process: the disk itself becomes unstable to collapse leading to the formation of numerous giant planets in 0.1 Myr or less (Boss 1998; 2002; Mayer et al. 2002). The simplest version of this model suggests a core mass of less than $10 M_{\oplus}$, but this value is rather uncertain, because any heavy element material forming the core must first pass through the fully formed envelope without dissolving (Helled et al. 2006). The early evolution of the solar system would have been very different for each of the formation scenarios, as would the number and nature of planetesimals captured by the giant planets. Present models for Jupiter's interior allow a range of zero to $12 M_{\oplus}$ for the mass of the planet's core (Guillot et al. 2004). Analysis of the Juno gravity and microwave observations will constrain both the core mass and the total mass of heavy elements, contributing to the resolution of this planetary formation question.

Because the measured gravity field of Jupiter is insensitive to the relative amounts of rock- versus ice-forming elements in the interior, one cannot constrain easily the rock-to-ice ratio in planetesimals from the gravity data. It is plausible that oxygen from water ice forms a significant fraction of the mass of Jupiter's core, since water ice is likely to be the most abundant condensate in the Jupiter-forming region. For example, Ganymede and Callisto are roughly half water ice, half rock by mass and are presumably representative of the late infall of solid materials in that region. The measured gravity field mainly constrains the amount of mass centrally concentrated in the core, not its density nor the details of how the mass within the core is distributed.

There are substantial differences between the two types of formation models, including formation timescale, favorable formation location, ideal disk properties for planetary formation, etc. Their differences naturally leads to some differences in planetary composition. However, the final composition of the planet formed by both models could change considerably depending on the local disk properties of the planetary birth environment. As a result, the size or presence/absence of a core—even a large one—does not by itself tightly constrain the conditions in the nebula where and when Jupiter formed. An accurate determination of Jupiter's composition can provide better constraints, in particular the pattern of enrichment of the heavy elements relative to solar composition in the envelope (partially obtained by Galileo probe; Wong et al. 2004) with the water abundance provided by Juno's MWR investigation.

2.2 Bulk Thermal Evolution and the Interior Structure

Further complexity in relating Jupiter's core mass to its formation is caused by the fact that Juno will reveal information on Jupiter in its current state, i.e., about 4.5×10^9 years after its formation. Planetary evolution during the billions of years subsequent to Jupiter's formation may have resulted in significant changes in its internal structure. Therefore, Jupiter's current structure may be quite different from its internal structure shortly after formation. For example, a large fraction of Jupiter's primordial core may have been eroded by convective eddies that carry heavy elements from Jupiter's core and remix them into the gaseous envelope (Guillot et al. 2004; Wilson and Militzer 2012). Convective mixing can lead to more homogeneous composition, whereas helium rain can alter atmospheric composition with time, depleting helium from the gaseous envelope. These physical processes demonstrate the need for detailed evolutionary interior modeling if we are to understand how Jupiter's internal structure as measured today relates to the structure during the formation process.

The basic idea behind interior modeling is to use an appropriate equation-of-state and the measured physical properties of the planet to obtain a density profile through the interior. The structure and evolution of Jupiter can be described using theoretical constraints on hydrostatic and thermodynamic structure plus mass and energy conservation. These constraints are dependent on the pressure, temperature and density. Then, the planetary composition and its depth dependence are determined, consistent with an understanding of the equation of state and evolutionary models. Since observations are used to constrain the interior model, the more observations we have, and the more accurate they are, the more detailed the derived interior model.

Several assumptions must be made in order to model the interior of Jupiter. Naturally, some assumptions are more justified than others, and the model assumptions will necessarily have various effects on the derived interior structure. The assumptions of interior models might be divided into simplifications/approximations and conjectures. While the first corresponds to assumptions like spherical symmetry and the absence of magnetic field, the second corresponds to a priori assumptions on the planetary structure such as nature of rotation, the planetary thermal structure, etc. The simplifications that are typically adapted for interior modeling besides spherical symmetry are a non-magnetic internal structure, and a solid-body rotation for the planetary interior that is included only in the representation of the planetary mean radius. The physical motivation for solid-body rotation is the likely role that the magnetic field has in suppressing large differential rotation for most of the mass (out to perhaps 95% of the radius). Indeed, the System III reference frame used for Jupiter is strictly that of the magnetic field.

Assumptions on the planetary internal properties include adiabaticity, the number of layers, the hydrogen to helium global ratio, and the materials from which the planets are composed—ices and rock in addition to the hydrogen and helium.

The total mass of Jupiter is the most constrained physical property. Other physical properties that are used by the interior model are the gravitational coefficients J_2 , the equatorial or mean radius, the temperature at the 1 bar pressure-level (which is used to determine the entropy of the planet), the rotation rate of the planet, and occasionally the atmospheric helium to hydrogen ratio $Y = (X + Y)$, where X and Y are the mass fractions of hydrogen and helium, respectively. The best information on Jupiter's atmospheric composition comes from the Galileo probe. The helium to hydrogen ratio was found to be 0.238 ± 0.05 , smaller than the protosolar value of 0.275 ± 0.01 , inferred from solar models. Since helium is found to be depleted in the upper envelope, interior models often divide the planetary envelope into a helium-poor outer region, and a helium-rich inner envelope. It is not known whether the heavy elements are homogeneously distributed within the planet.

The rotation rate of the planet is also required to model the interior. For Jupiter, most interior models use the System III rotation period (Bagenal et al. 2017, this issue) that is determined from periodic variation of radio emissions from Jupiter, observed over many decades. The modulation of jovian radio emissions is due to rotation of its magnetic field, assumed to be the same as the rotation of the deep interior where the magnetic field is generated.

Jupiter emits more energy than it receives from the Sun (e.g., Low 1966) indicating that Jupiter is still cooling and contracting. The Virial theorem tells us that the source of Jupiter's luminosity is the decrease of internal heat content, primarily. There is a concomitant decrease in gravitational energy due to contraction, which is, however, balanced by the work done compressing the materials to higher pressure in the deep interior (Hubbard 1968, 1977). Jupiter's radius shrinks at a rate of 3 cm/year. The atmospheric temperature at the 1 bar pressure-level is often used as a boundary condition for interior models. More precisely, the interior models assume an isentropic structure (often referred to as adiabatic) and so the specific entropy at 1 bar is about the same as the specific entropy deep within the planet, provided there are no intervening phase transitions or compositional jumps. For Jupiter, the temperature at 1 bar has been measured by the Voyager spacecraft to be 165 ± 5 K (Lindal et al. 1981). However, this temperature was derived using the ratio of hydrogen to helium as it was known at that time. The temperature at 1 bar is higher by about 5 K using the updated value of Jupiter's atmospheric hydrogen to helium ratio measured by the Galileo probe. Yet these temperature estimates are based on radio occultation measurements, whereas the Galileo probe measured a temperature of 166.1 ± 0.4 K (Seiff et al. 1998). The Galileo probe evidently entered a hot spot, a region that may not be representative; the temperature estimates should be adopted with a bit of caution.

The assumption of isentropy stems from two considerations: (1) the prevalence of convection as the means of carrying heat from the interior, and (2) the smallness of the deviation from isentropy (i.e., the very small gradient of entropy with pressure) that is sufficient to carry that heat by convection, given the very low viscosity. The argument for convection in the deep atmosphere is based on the insufficiency of radiative heat transport due to the increase of opacity with depth for molecular hydrogen. However, other constituents are needed to guarantee sufficient opacity in the region around 1200–2000 K, probably alkali metals (Guillot et al. 2004). It is also straightforward to show that thermal conduction is insufficient to carry the observed heat flow, even in the deep interior.

Isentropy could in principle allow one to determine the temperature at the center of Jupiter given the temperature at one bar. However, this is contingent on the absence of layering. The question of whether Jupiter is somehow layered is a complex one and not resolved (and may not be fully resolved by Juno). One way of producing layering is a phase transition, and indeed the condensation of water and rock-forming elements, which are first order phase transitions of minor elements, are examples of where a small amount of layering is assured. The only deep first-order phase transition that is likely under jovian conditions is the limited solubility of helium in hydrogen, once hydrogen becomes at least partly metallic. There is currently no evidence that the metallization of pure hydrogen is a first-order (or indeed any order) phase transition at the temperature of relevance in Jupiter; it is instead gradual and therefore would not result in layering (cf. French et al. 2012). However, the dependence of helium insolubility on metallization may lead to a layering that occurs at a region similar to that where hydrogen metallizes, of order a megabar but with a large uncertainty still.

Another way of producing layers assumes the planet was built inhomogeneously (e.g., by forming a core first) and then imperfectly homogenizing by later convection. An inhomogeneous composition may occur as a result of mean molecular gradients leading to a

“layered convective” interior (Baraffe et al. 2008; Leconte and Chabrier 2012). In that case, the amount of high-Z material in the planetary atmosphere does not represent the global enrichment of heavy elements throughout the entire planet. Quantum mechanical calculations (Wilson and Militzer 2011, 2012) show that all of the elements (other than helium) can dissolve in hydrogen at high pressure, so this kind of layering can only persist because of the inefficiency of convective mixing (i.e., the limited work that can be done by thermal convection). The fundamental constraint on this is that the gravitational energy of the planet must decrease (i.e. become more negative) with time, but this is compatible with doing the work required to mix the core up into the overlying hydrogen, since cooling from an initial hot state is a large reduction in gravitational energy, especially in the first tens of millions of years after accretion.

As noted above, the simplest interior models assume rigid body rotation. However, differential rotation, if it involves a sufficient amount of mass, can contribute to the gravitational harmonics (Hubbard 1999). As a result, any uncertainty in the nature of rotation in Jupiter results in an uncertainty in the derived internal structure. Juno will determine Jupiter’s gravitational harmonics up to degree 12 and will therefore provide constraints on the contribution of the dynamics to determination of the internal structure. With this additional knowledge, interior models can include the effect of the planetary rotation, and provide more accurate determination of the planetary interior.

In addition, one has to make assumptions regarding the heavy-element enrichment of the envelope and/or on the properties of the core. It is known that Jupiter is enriched in heavy-elements compared to the Sun, but the exact enrichment, as well as the distribution of the heavy elements within the planetary interiors are not known.

2.2.1 Equation of State and Other Thermodynamic Issues

Jupiter consists of mostly hydrogen (H) and helium (He), and a smaller fraction of heavy elements (elements other than hydrogen and helium, with relative mass fraction Z). As a result, interior models of Jupiter rely strongly on the equation of state (EOS) of hydrogen, helium and their mixture. Deriving an accurate EOS for the entire pressure and temperature regime of Jupiter is very challenging. First, in some regions atoms, ions, and molecules co-exist and interact. For the high temperatures and pressures a great effort to determine the EOS of hydrogen has been carried out both in laboratory experiments and theoretical models. Laboratory experiments have great difficulty in approximating the conditions relevant to the interiors of the giant planets. Typically, shock wave experiments are too hot at the relevant pressures and diamond cell experiments are too cold at the relevant pressures. At present, the equation of state of hydrogen is well determined for densities and pressures less than about 0.3 g cm^{-3} and 0.25 Mbar, respectively, using gas-gun shock experiments (see Saumon and Guillot 2004, for details). For higher densities and pressures the experiments cannot provide very accurate determinations due to fairly large errors, and therefore more accurate experiments are required in order to provide a more complete picture on the behavior of hydrogen at high pressures and densities.

An alternative method to determine the equation of state at the high pressure/density regime is to use theoretical equations of state. There are two main theoretical approaches for determining the EOS that are used in astrophysics, the chemical approach and first principles numerical simulations. The first method takes the mixture of molecules, atoms, ions, and electrons, then, by using the free-energy approximation, the thermodynamic variables of the material are determined. The chemical approach accounts for the interactions between the different components of the materials but cannot cover all the interaction in the system. As

a result, chemical models are not able to provide accurate predictions in the coupled regime where interaction effects are more important than the kinetic effects, and at high-density regimes chemical models must be completed using other data (see Saumon et al. 1996 for details).

First-principles numerical simulations are based on the fundamental properties of electrons and the nuclei and are independent of experimental or other theoretical data. These computer calculations essentially simulate the behavior of hundreds of particles at various pressure and temperature regimes. In the context of planetary modeling, the first principles simulations that are used are the density functional molecular dynamics (DFT-MD).

Jupiter also consists of materials heavier than helium, albeit in relatively low abundance. Ices or rocks represent the heavy elements in typical interior models. Although the equation of state of the heavy materials has only a small impact on the derived internal structure, constraining the amount and distribution of heavy elements within Jupiter has important implications for our understanding of planetary formation and evolution. Heavy elements in Jupiter's interior are often assumed to be homogeneously mixed within the hydrogen/helium envelopes due to efficient convection, but as noted above, it is possible to imagine a Jupiter that is stably layered with an outward decrease in the heavy element mixing ratio. More details on equation of state calculations can be found in Fortney et al. (2011), Guillot (2005) and references therein.

Helium is depleted in Jupiter's atmosphere, compared to the protosolar value, and perhaps even more depleted in Saturn's atmosphere (e.g., Von Zahn et al. 1998; Conrath and Gautier 2000). It has been suggested (Stevenson 1975; Stevenson and Salpeter 1977; Fortney and Hubbard 2003, 2004) that the depletion of helium in Saturn's (and Jupiter's) atmosphere is a consequence of helium separation from hydrogen. If helium becomes insoluble in hydrogen, it can coagulate to form helium droplets that settle towards the planet's center (due to larger density). Helium separation provides an explanation for the low helium abundance in the atmosphere, and it also offers an additional energy source that seems necessary to explain the long-term evolution of Saturn (Fortney and Hubbard 2003).

Enrichment of high-Z material is measured in Jupiter's atmosphere (2–3 times the solar value), and although interior models predict global enrichment of heavy elements (typically 10 to 20%) as noted above it is not known how the high-Z material is distributed within the planet's interior.

2.2.2 *Fitting the Data with Models*

Interior models of Jupiter have been developed over several decades. Below, we summarize results from fairly recent interior models. Guillot and collaborators (Guillot et al. 1997; Guillot 1999; Saumon and Guillot 2004; Guillot 2005) have presented interior models of Jupiter using a three-layered structure. These models provide estimates of Jupiter's core mass as lying between zero and $10 M_E$ (Earth masses). In 2008, two independent groups modeled Jupiter's internal structure using the first-principles equations of state. Militzer et al. (2008) simulated the H/He mixtures directly and found a massive core for Jupiter with masses between 14 and $18 M_E$, and suggested that Jupiter's envelope is depleted of water (H_2O) with most of the water being deeper in the interior, closer to the core. In this model, Jupiter is found to be fully convective with an envelope of homogeneous composition. While this model fits Jupiter's measured J2, in order to fit Jupiter's measured J4, differential rotation on cylinders has to be imposed, therefore suggesting that Jupiter may not be rotating as a solid-body. Juno will be able to constrain the water abundance in Jupiter's atmosphere as well as the "depth" of differential rotation, allowing the validity of the water-depleted interior model to be tested

The model derived by Nettelmann et al. (2008) also assumed that Jupiter's interior can be represented by three layers: a core, a heavy-element enriched metallic region, and a heavy element depleted molecular envelope, similar to the models of Guillot. The equation of state was derived separately for the different materials (i.e., H, He, H₂O), and the thermodynamic properties of the mixture was derived including their relative contributions. Following Guillot (1999), they assumed that the upper envelope is depleted in heavy elements compared to the inner metallic envelope. The derived interior model suggests a small core mass with a heavy-element enrichment similar to the one found by Saumon and Guillot (2004). Clearly, the models of Militzer et al. (2008) and Nettelmann et al. (2008) differ in the assumed internal structure (two- vs. three-layers), the treatment of the EOS, and in the temperature profiles. Detailed investigation of the difference of the two models can be found in Militzer et al. (2008). Recently, Leconte and Chabrier (2012) have investigated Jupiter's internal structure assuming an inhomogeneous distribution of heavy elements. With this configuration, the interior is no longer adiabatic, invalidating the isentropic assumption about the interior. As a result, the internal temperatures are higher than those of an adiabatic interior. In this model, the total heavy-element mass is significantly larger than in other models, and was found to be up to 63 M_E with no (or very small) core. This work clearly demonstrates the strong effect of the model assumptions on the derived internal structure, and the consequences of the simple assumption of an adiabatic and homogeneous planet.

2.3 The Importance of the Internal Magnetic Field

Jupiter's magnetic field is over an order of magnitude larger than Earth's field. Previous missions have established a crude map (out to fourth harmonic degree), the most recent (pre-Juno) version of which was Connerney et al. (1998). Unlike the static gravity field, the magnetic field offers the possibility of learning about the dynamics deep within Jupiter, because the only known way of sustaining the field is through a dynamo process that depends on the motions of an electrically conducting fluid. For example, the existence of Earth's magnetic field is attributed to convective motions in earth's liquid iron outer core and this in turn places constraints on the heat flow out of the core and thus the cooling rate of Earth. In a giant planet such as Jupiter, large scale convection is easily accomplished provided the fluid is homogeneous over a substantial radial extent, and adequate conductivity is possible once the hydrogen begins to metallize. Even a rather poor metal or semiconductor may suffice provided the fluid motions are sufficiently vigorous and large scale. The relevant parameter characterizing a dynamo is the magnetic Reynolds number,

$$R_m \equiv vL/\lambda$$

where v is a characteristic fluid velocity (must include a vertical component since rigid body rotation or even differential rotation does not suffice), L is a characteristic scale (size of the convecting region) and the magnetic diffusivity $\lambda \equiv 1/\mu_0\sigma$ where μ_0 is the permeability of free space and σ is the electrical conductivity (units of S/m). A value of R_m exceeding ~ 10 or 100 is typically required for a sustained dynamo (see discussion in Stevenson 2009). For example, if $v \sim 10^{-2}$ m/s (a plausible value of the convective vigor given Jupiter's known heat flow) and $L \sim 10^7$ m, we need σ in excess of 100 or 1000 S/m. A typical good metal is $\sim 10^6$ S/m while salty water is only 1 S/m. The needed conductivity is obtainable out to perhaps 0.91 or even 0.93 of Jupiter's radius (French et al. 2012), but of course all the parameters in this assessment (including the critical R_m) are somewhat uncertain. Juno is expected to find roughly the radius at which the conductivity is sufficient for field generation, by looking at how the power spectrum decays with harmonic degree, since it is known

that dynamos have rather flat power spectra within the dynamo region but higher harmonics decay much more quickly than low harmonics with radius outside the dynamo region. However, there is potentially much more information that is likely to be obtained about the nature of dynamos in general (since Juno can get better data for Jupiter than we have for Earth's core) and about the scale and character of the flows responsible for generating the field. If the mission continues long enough then there is the exciting possibility of seeing a change in the field (the means whereby Edmund Halley first deduced that Earth's field is dynamic rather than a mere bar magnet). There is also the possibility of seeing how the differential rotation in the outer regions of the planet may affect the field.

2.4 The Importance of Water and Heavy Element Enrichment

The measurement of the water abundance of Jupiter is pivotal in understanding giant planet formation and the delivery of volatiles throughout the solar system. This follows from the fact that oxygen is the third most abundant element in the universe and icy planetesimals were the dominant carriers of heavy elements in the solar nebula. The deep oxygen abundance in Jupiter was not known prior to Juno because the abundance of water—the primary carrier of oxygen in the jovian atmosphere—is in principle strongly affected by condensation and rainout associated with meteorological processes (Lunine and Hunten 1987), by advection (Showman and Dowling 2000), or both. This seemed to be demonstrated by the outcome of the Galileo probe descent through Jupiter's atmosphere; it fell into a relative dry region known as a “5- μm hot spot” (for the excess brightness observed in such regions at 5 μm wavelengths), and the water abundance was observed to increase with depth, or equivalently, with pressure (Wong et al. 2004). The sparseness of the measurements makes it impossible to know whether the water has “leveled out” at a value corresponding to 1/3 solar or would have increased further had the probe returned data below the 22-bar level where communication ceased. It is assumed by most but not all authors (e.g., Lodders 2004) that the water abundance continues to increase with depth beneath this level, finishing at a value equivalent to an oxygen (O) abundance relative to hydrogen that is above the solar value, that is, “supersolar” (e.g. Mousis et al. 2012). Conversely, the carbon enrichment is well determined for Jupiter as lying between 3 and 5 times solar (Wong et al. 2008). Thus, the abundance of O relative to other heavy elements in Jupiter—provided it can be determined—tells us something about the conditions in which the planetesimals which contaminated the jovian envelope with heavy elements were formed.

For example, if water were found to be enriched in similar proportion to nitrogen, carbon, sulfur, and the noble gases (~ 3 times solar), a model producing planetesimals from ice that condensed at less than ~ 30 K (cold) would be favored (Owen et al. 1999). This could require inward migration of core-forming planetesimals, or Jupiter itself (Alibert et al. 2005), from much larger distances or a model of the formation of the solar nebula that includes the direct transfer of interstellar material in large agglomerations. If water is much more enriched than the noble gases, i.e., by 9 or more relative to solar, then the trapping of noble gases would be more characteristic of that expected through formation of planetesimals from ice grains that condensed at ~ 150 K near Jupiter's present location with subsequent cooling to 35 K (Gautier et al. 2001; Hersant et al. 2004). Because these planetesimals may have been the most abundant solid material in the early solar nebula, they therefore may also have been important to the delivery of volatiles to the inner planets (Owen and Encrenaz 2003). The Juno microwave radiometry investigation determines the water abundance in Jupiter at about the 100 bar level (Janssen et al. 2017), and because it maps the water over all latitudes, it is not prone to the sampling bias by measurements at one or a few probe locations as Galileo

was. Juno will provide a major step toward completing the inventory of ices and refractory material present in the early solar system and constraining planet formation scenarios.

2.5 Dynamical Processes in the Atmosphere

The depth of the major flow features is the most basic question of jovian meteorology. The objectives of the Galileo probe mission were to measure composition, temperatures, winds, clouds, lightning, and radiative heating from the top of the ammonia cloud at ~ 0.5 bars to below the base of the water cloud, which was expected to lie at ~ 5 bars for a solar abundance of water. There it was supposed to sample the well-mixed interior of Jupiter. These measurement objectives were derived from an atmospheric model that neglects large-scale motion below the clouds. The probe survived to 22 bars, but evidently did not reach the well-mixed interior.

Based on remote-sensing data, the probe entered a dry spot, a so-called 5- μm hot spot. The surprise was that the roots of the hot spot extended down at least to the 22-bar level, 150 km below the tops of the visible clouds. These deep roots are apparently part of a large-scale dynamical structure. One theory is that the hot spot is a giant downdraft extending 150 km below the ammonia cloud layer (Atreya et al. 1999); another theory is that it is the trough of a giant wave with vertical displacements of 150 km (Showman and Dowling 2000). There are other possibilities. For instance, 99.9% of the planet might look like a hot spot, with the saturated updrafts concentrated in a few violent thunderstorms occupying 0.1% of the area. Jupiter has no solid or liquid surface, so the dynamical structures could extend to 100 bars or deeper.

The dozen or more pairs of dark and light bands that circle the planet on lines of constant latitude are called belts and zones. The high-speed jets are on the boundaries. The prevailing view, based on clouds and chemical tracers, is that the belts are sites of downwelling, but the concentration of lightning in the belts (Gierasch et al. 2000) seems to contradict this view. Individual belts, zones, and ovals have persisted for over 100 years. This longevity is remarkable given that Jupiter is a fluid planet with no solid surface to provide stability. Deep roots and their large inertia may be the key to this longevity (Busse 1976; Ingersoll and Pollard 1982).

Juno produces pole-to-pole latitudinal maps of microwave opacity as a function of altitude to depths greater than 100 bars. The independent swaths at different longitudes and ability to target large-scale features near close approach provide the ability to understand large scale features such as the Great Red Spot. The 0.1% precision of the radiometer allows us to measure small variations in radiance with respect to horizontal position and emission angle, and to separate the effects of water from those of ammonia. With these measurements, we determine the global O/H and N/H ratios; we correlate the patterns of ammonia and water abundance below the clouds with the principal dynamical features at cloud-top level; we examine the deep roots of features like the Great Red Spot, the belts and zones, and potentially the 5- μm hot spots; and we quantify the role of latent heat processes (cloud formation, lightning) in the transport of energy in Jupiter's atmosphere. Context for these features is provided through coordinated Earth-based images and comparison with data from the Juno-Cam imager and the Jupiter Infrared Auroral Mapper (JIRAM) near-infrared instrument.

Hot spots are regions on the disk of Jupiter where infrared radiation escapes from relatively deep pressure levels. Such features are thought to be areas of dry air that result from regional downwelling or subsidence (Adriani et al. 2008). While larger hotspots tend to occur in the North Equatorial Belt "excess" thermal radiation is seen from much of the planet and may indicate a complex pattern of cloudy versus dry air. The JIRAM instrument performs co-located spectroscopic and imaging observations of selected regions of Jupiter's

atmosphere in the broader 2.0–5.0 m wavelength range with moderate spectral resolution (Adriani et al. 2017). JIRAM provides information on hot spot structure and chemistry, mapping the abundances of a number of major and trace species with high spatial resolution as high as 10 km, and depths approaching 10 km.

With Juno, we can observe dynamically distinct regions of the planet over a range of depths and with large spectral coverage. At cloud-top level (pressure 0.5–1.0 bar), the banded appearance of the planet gradually gives way to a mottled appearance at latitudes above $\pm 65^\circ$, signaling a fundamental change in the dynamics. A high-altitude haze covers the regions poleward of $\pm 65^\circ$. Whether this haze is related to bombardment by charged particles from above (auroral chemistry, observable by JIRAM and UVS) or to the atmospheric dynamics below is uncertain. Constraints of celestial mechanics and limited heat-shield technology make it impossible with current and foreseeable technology to put an instrumented probe into the polar regions of Jupiter. However, JIRAM samples the polar troposphere down to 10 bars and MWR to depths greater than 100 bars. If there is a fundamental equator-to-pole change in the dynamics of the troposphere, and if that change is mirrored in the ammonia and water mixing ratios, or in the temperature structure, Juno's atmospheric sounding capabilities will quantify it.

Early in mission planning, it was decided to promote a robust campaign of Earth-based observational support for the mission in order to extend and enhance Juno's scientific output. This campaign supplements Juno's capabilities in four ways. (i) This support campaign provides a global context for Juno's remote-sensing of Jupiter's atmosphere, which is dominated by high-resolution observations in discrete regions of the atmosphere. For examples of context images see Fig. 20 of Janssen et al. (2017, this issue) for the MWR instrument, or Fig. 30 of Hansen et al. (2017, this issue). (ii) The campaign provides a temporal context for Juno's observations by tracking the evolution of individual features that are measured by Juno instrumentation at one point in time. (iii) The campaign supplements Juno's spectral coverage by observing Jupiter at wavelengths not included in Juno's own instrumentation, such as the X-ray or mid-infrared. (iv) The campaign also provides simultaneous coverage of multiple components of the jovian system that influence Juno's measurements. One example is measurements of Io's volcanic activity that ejects material into and influences various properties of Jupiter's magnetosphere.

The campaign consists of over 60 individual observing groups using ground-based, Earth-orbiting and Earth-proximal observing platforms measuring a broad spectral range from X-ray to the radio. A web site (<https://www.missionjuno.swri.edu/planned-observations>) tabulates the details of these observations and is updated in real time by the Juno and supporting scientists, mirroring the contents of an interactive site maintained by the investigators.

2.6 Dynamical Processes in the Magnetosphere

Juno is the first spacecraft in polar orbit around Jupiter allowing it to venture deep into the unexplored polar regions of the magnetosphere, as reviewed by Bagenal et al. (2017, this issue). The spacecraft trajectory and instrument complement provide Juno with the tools to tackle the key scientific questions involving the jovian aurora (spatial and temporal structure, generation processes, relationship to magnetospheric processes), the synchrotron radiation belt (spatial and temporal structure, source and loss processes) and plasma sheet (spatial and temporal structure, relationship to aurora, particle acceleration processes). Moreover, the approach and apojoVe sections of the first dozen orbits provide valuable opportunities for Juno to quantify the solar wind interaction with boundary layers on the dawn side.

Subsequent to the preparation of the Bagenal et al. (2017, this issue) review, the decision to keep the Juno trajectory in a 53-day orbit resulted in a significant change to the mission plan. Here we provide updated illustrations of how the current trajectory changes the magnetospheric science that Juno addresses.

Figure 3b shows Juno's trajectory with the 53-day orbit, as viewed from the Sun, and Fig. 3a looking down on the equator. This figure replaces Fig. 6 (bottom and top, respectively) of Bagenal et al. (2017, this issue). Figures 3a, 3b, 3c, 3d show the locations of the magnetopause (MP) and bow shock (BS) derived by Joy et al. (2002) based on combining previous spacecraft measurements and an MHD model. The average MP and BS distances (close to the equator on the dawn flank) are $105 R_J$ and $165 R_J$ respectively with the 10th to 90th percentile ranges shaded ($85\text{--}145 R_J$ for the MP and $130\text{--}230 R_J$ for the BS). Juno crossed these boundaries several times on the approach and during the capture orbit as predicted by Ebert et al. (2014). A mission plan that retains the 53 day orbit with apojove at $113 R_J$ provided many more BS and MP crossings on subsequent orbits until the orbit local time clocked around towards midnight. A further advantage of the large orbit means that Juno will spend considerable time in the tail of the magnetosphere (see Fig. 2 of Bagenal et al. 2017, this issue) and will likely cross the X-line (where material is ejected down the magnetotail) multiple times. Finally, Fig. 3b shows that there is a possibility that Juno will cross the magnetopause again towards the very end of the emission, particularly if the magnetosphere is more flattened than predicted by the Joy et al. (2002) model.

Figures 3c and 3d show how Juno's trajectory evolves southward with time, with the inbound equator crossing moving inward towards Jupiter. This will allow Juno to map out the magnetospheric structure between $15\text{--}100 R_J$ on the nightside of Jupiter. While the Galileo spacecraft also covered this region at low magnetic latitudes (see Fig. 4 of Bagenal et al. 2017, this issue) the instruments on Juno have a far higher sensitivity and temporal resolution.

Bagenal et al. (2017, this issue) chose three orbits to illustrate the changing geometry of the orbit through the mission: PJ3, PJ17 and PJ31 (see their Figs. 7, 13, 14, 15, 16). While the apojoves of these orbits are very different with the current 53-day orbits, the perijove sections of the orbits are very similar. Nevertheless, the specific longitudes and magnetic geometries are rather different and these orbits are now spaced two years apart (in December of 2016, 2018 and 2020). In Fig. 5 we show the current Juno trajectory for these same three perijoves in magnetic coordinates where the spacecraft oscillates in latitude due to the $\sim 10^\circ$ tilt of Jupiter's magnetic dipole. Figure 5 illustrates the effect of the southward progression of the orbit giving Juno increasingly better coverage of the plasma sheet on the inbound leg and increasing time spent over the south polar region on the outbound leg.

In Fig. 6 we show the Juno trajectory projected along the magnetic field using the VIP4+CAN model (see Juno MAG paper by Connerney et al. (2017, this issue) onto the 1-bar level of Jupiter's atmosphere, including the polar flattening of the planet. This model uses a 4th degree and order spherical harmonic expansion for the internal magnetic field (Connerney et al. 1998) combined with an explicit model of the magnetodisc (Connerney et al. 1981) representing the external field. The average location of the main auroral emissions, as observed by the Hubble Space Telescope (Grodent et al. 2003; Bonfond et al. 2012) are shown for reference. Again, the progression of Juno's orbit through the mission results in the spacecraft moving to increasingly lower (higher) latitudes in the north (south). This provides multiple passes at a range of altitudes of Juno (carrying instruments that measure in situ particles and fields) through magnetic field lines connected to the main aurora, as well as considerable coverage of the polar auroral regions, particularly in the south. At the same time, Juno's UVS and JIRAM instruments will be observing the UV and IR auroral

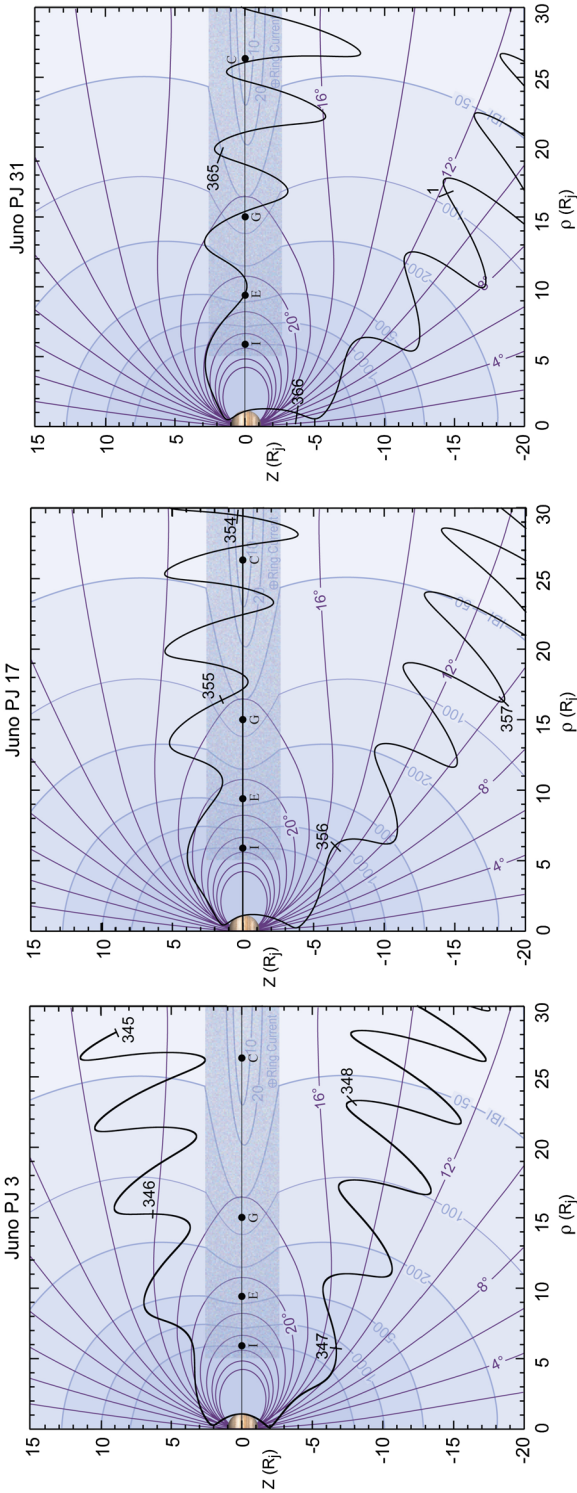


Fig. 5 Juno's orbit plotted in magnetic coordinates (using the VIP4+CAN model). We show three orbits typical of the beginning (PJ3), middle (PJ17) and end (PJ31) phases of the mission to illustrate how the effect of the orbit precession changes the spacecraft trajectory through the equatorial plasma sheet. Fiducial field lines (*purple*) are shown for magnetic co-latitudes every 2° from the magnetic pole to 30° and magnetic field magnitude is shown by *blue contours* in units of nT. Tick marks are shown at day-of-year boundaries

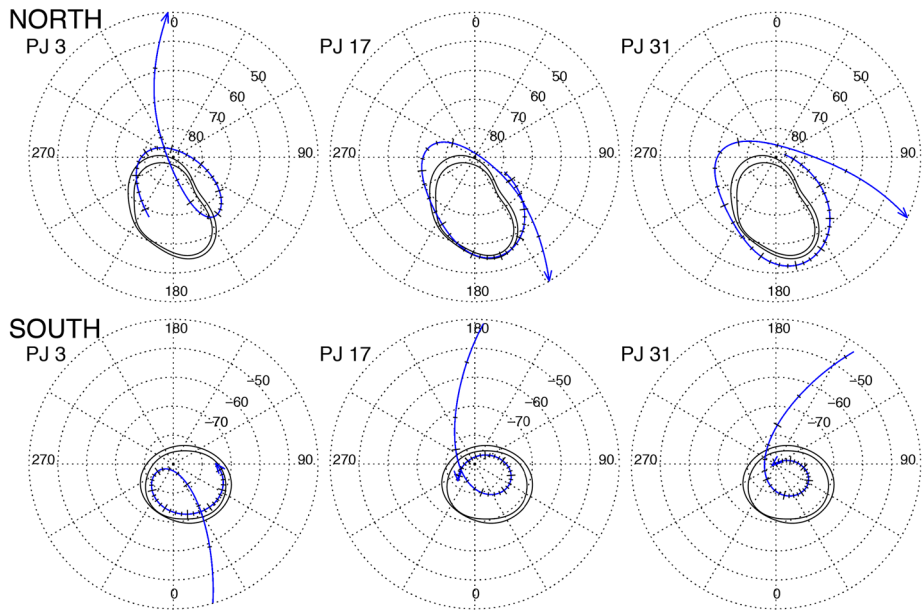


Fig. 6 To illustrate how Juno traverses the auroral regions, the trajectory is projected down onto the planet along the local magnetic field (using the VIP4+CAN model). In this coordinate system that is fixed to Jupiter's spin, the Juno trajectory moves through increasing longitude with time. We show three orbits typical of the beginning (PJ3), middle (PJ17) and end (PJ31) phases of the mission to illustrate how the effect of the orbit precession changes the relationship of the spacecraft trajectory to the average auroral oval (shown with double black lines). North (south) trajectory plots start (end) when the spacecraft is $10 R_J$ away with tick marks every 10 minutes

emissions. Bagenal et al. (2017, this issue) describes how Juno's combination of in situ and remote sensing measurements of Jupiter's aurora (the quasi-steady main aurora, the highly-variable polar aurora and satellite aurora triggered by Io, Europa and Ganymede), test theoretical ideas about their generation mechanisms, and compare with the auroral processes observed at Earth.

3 Juno Science Operation Center

The Juno Science Operations Center (JSOC) provides a central organization and data system to the Juno team to facilitate science planning, data distribution, data archiving and provide support functions. The JSOC system and its processes have evolved to meet the need of the Juno science and operations teams. JSOC data system's integrated web application allows access to the system from any internet accessible location without the need for special client software. The JSOC data system provides three major functions: Science Planning, Data Management, and Meetings and Documents. The Juno operations team uses the Science Planning module to create validated activity plans for execution with ease of use and efficiency by enabling use of templates, copying of instrument activities and instant validation functionality. All instrument data within JSOC is PDS compliant, and can be tagged, shared within the team and delivered to PDS by using features available on the website using the Data Management module. The Meetings and Documents module provides means to share

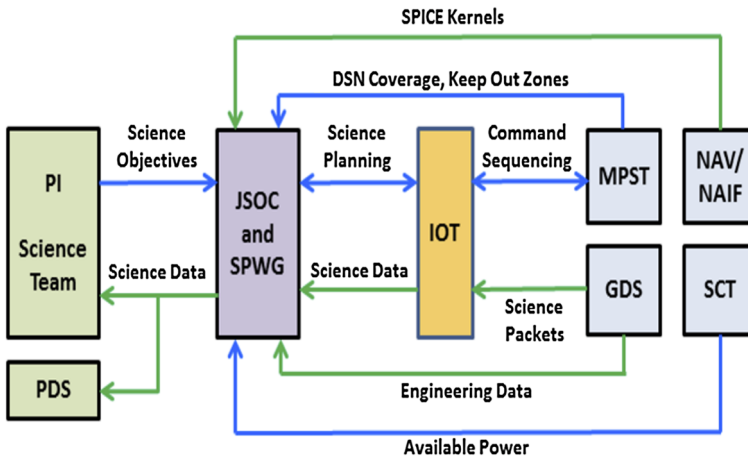


Fig. 7 Data flow and relationships between entities involved in Juno science operations and data management. The entities are Juno Science Operations Center (JSOC), Principal Investigator (PI), Science Planning Working Group (SPWG), Instrument Operations Teams (IOT), Mission Planning and Sequencing Team (MPST), Navigation Team (NAV), Navigation and Information Facility (NAIF), Spacecraft Team (SCT), Ground Data System (GDS) and the Planetary Data System (PDS)

presentations, documents and files in the same system as rest of science operations. Many tasks that were previously manually performed have been automated, thereby reducing the risk and complexity of operations.

3.1 JSOC within the Juno Mission Operations System

The Juno Science Operations Center (JSOC) is the center for science planning and data distribution for the Juno mission. It is a component of the Juno Mission Operations System (MOS) and interacts with other MOS components, the Juno science community and the Planetary Data System (PDS). Figure 7 shows relationships and data flow between the various entities. The PI, science team and the instrument teams provide science activity inputs to the planning process. The Mission Planning and Sequencing Team (MPST) provides data volume constraints, instrument activity keep out zones (KOZ), and performs sequence validation. The Spacecraft Team (SCT) provides power constraints and the navigation team (NAV) produces SPICE kernels necessary for planning activities and analyzing science data and delivers to the Navigation and Information Facility (NAIF) that administers SPICE. JSOC provides science planning support, generates science activity plans (SAPs) that form inputs to the Instrument Operations Team (IOT) sequence generation process. Additionally, JSOC facilitates science and engineering data storage, dissemination and archiving, and provides supporting tools for meetings and document sharing within the Juno team. The Instrument Operations Teams (IOTs) generate command sequences, perform instrument state-of-health assessment, process data and perform science analysis. The Science Planning Working Group (SPWG) comprises representatives from all these entities (and is co-chaired by two science team members) is tasked with coordinating the science priorities, science trade-offs, instrument activities, and approving the resulting SAP. To facilitate science operations, JSOC has created an integrated web-based data system.

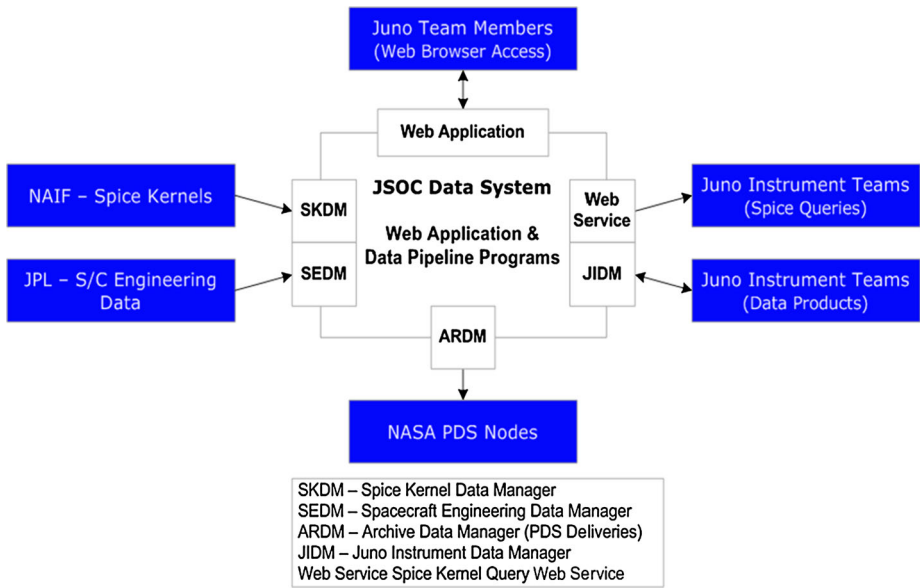


Fig. 8 JSOC data system components and interactions with external entities

3.2 The JSOC Data System

The JSOC Data System (DS) is an integrated, web-database system that provides access to extensive science planning, data management, and meetings & document functions for scientists, engineers, operations and management personnel across the Juno mission through any recent web browser or web-enabled device. It is designed as a High Availability system with two instances of the database online simultaneously providing failover capability. It has automated data pipelines, PDS delivery functions, and web services that provide seamless data transfer functions, enhance science planning and instrument operations, and increase the efficiency of archiving activities.

The JSOC DS was first released in beta form in January of 2010, and has been expanded and optimized through subsequent years. Many of the typical SOC functions in JSOC DS have been through several versions of enhancements. Extensive mission-customized data volume and power modeling functions are utilized by the Juno team in mission planning and operations.

The central component of the architecture is the JSOC web application which consists of connecting to an Oracle Real-Time Application Cluster (RAC) database. Four additional data pipeline programs provide automated transfer and processing of instrument data, PDS deliveries, spacecraft engineering data and SPICE kernels. A summary of the data system components that comprise the JSOC DS architecture is found in Fig. 8.

3.3 Capabilities

3.3.1 Science Planning Capabilities

One of JSOC’s primary functions is to streamline the Science Planning process, making it as efficient and effective as possible, while providing a significant level of detail for the

instrument teams and Science Planners to understand what the instrument teams want to accomplish and the amount of resources that will be used by producing charts, graphs, and data sets. The JSOC DS provides capability for multiple scenarios per time period, complete set of instrument requests per SAP with epoch-based times, data volume and power modeling for each SAP that may use different modeling algorithms, and document attachment and history functions for all of the above. Additionally, the system also has electronic approval functions and email notifications for SAP promotions.

The SAP is the primary object for modeling and planning. Multiple SAPs can be created for an Activity Period (AP) to allow testing of multiple data volume and power scenarios. This provides opportunities to optimize data return and fulfill science objectives.

3.3.2 Data Management Capabilities

The JSOC Data System contains data management applications that download, transfer, and process data. These programs receive data from instrument teams, verify PDS compliance of those files, build and deliver archive volumes to PDS, and distribute data to the Juno team. Additionally, they process spacecraft engineering data and SPICE kernels. A web service provides SPICE kernel lookup functions to enable automation of instrument data pipelines. These programs are monitored by status monitoring scripts to ensure nominal performance and generate alerts if system problems are detected.

3.4 Facilitating Juno Science Operations

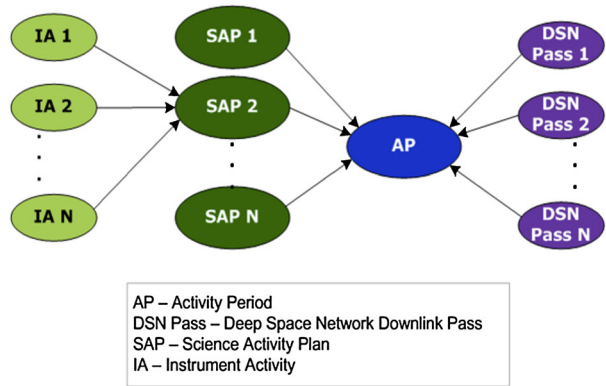
3.4.1 Science Planning Process

The JSOC works in close cooperation with the SPWG in creating validated and approved Science Activity Plans using the JSOC data system. An SAP is a detailed plan for an orbit or sequencing period and forms the basis of Juno's payload operation. Instrument Activities (IA) are the building blocks that make up the Science Activity Plan and describe instrument operations to be carried out for achieving a science objective or an engineering objective as well as the predicted resource use. They also include other attributes that need to flow down to sequencing. The SAP includes epochs that help define science collection periods and other useful times based on the trajectory, and Keep Out Zones (KOZs), the periods during which instrument operations are restricted due to spacecraft engineering activities. Each SAP has an Activity Period (AP) upon which the SAP is built. The AP defines plan boundaries and contains the resources available to the payload along with supplementary information like data volume margins and priority downlink periods for the sequence. See Fig. 9 for graphical reference. During cruise phase, each sequence was 28 days in duration and in the orbital phase, each 53-day orbit is divided into two sequences that may be of different durations. The AP also specifies the sizes of on-board memory partitions available to each instrument. The SAP and AP are implemented in the JSOC data system as a collection of database tables and relationships. Users can attach files to IAs, SAPs or APs for reference. The JSOC data system provides a number of views and export options for the SAP which are specific to various uses.

3.4.2 SAP Validation

Validation routines perform several checks on the SAP and can be done by any user simply by clicking a button. During validation, individual activities are checked to determine whether they have valid start and end times within the AP boundaries. A power model which

Fig. 9 Relationship between DSN passes, activity periods, science activity plans and instrument activities



computes aggregate power usage and determines whether the values exceed the available power is also executed. If there is a power deficit, the use of energy from the battery and subsequent recharging of the batteries is also modeled. The JSOC data system also has a data volume model which seeks to replicate the flow of data in and out of the spacecraft framed partition memory for each instrument based on inflow of data during collection periods and outflow during downlinks. The downlink priorities for each partition are controlled using flight software global variables which are set by the JSOC. Within the JSOC data system, these are called Fractional Data Allocation (FDA) sets and can be manually set by the JSOC science planners or can be computed by the software using an algorithm that uses proportional data production. The validation routines also identify periods of potential partition overflows, periods approaching the limits, as well as data volumes leftover at the end of the AP to be carried over into the following sequence. These are displayed in table form as well as in the form of charts for each instrument and as shown in Fig. 10, a validation summary chart that displays data volumes, instrument activities, epochs, DSN passes, available and used power, power margin and energy deficit. Figure 10 uses validation chart for the JM0051 SAP that includes a part of the orbit containing perijove 5 as an example.

An SAP can be versioned and have one of four states in order of progression—(1) Trial, where the SAP can be created and edited by any user to evaluate different options, (2) Draft, which is the official working SAP for a sequence with restrictions so that only instrument teams can edit their activities, (3) Pending, which prevents addition or deletion of instrument activities and editing of fields that influence power usage as and (4) Approved, which is a completely locked and approved SAP that is intended to be the source for flight activities.

3.4.3 SAP and Sequence Development Process

The PI and SPWG provide input to the mission planning process and identify targeted perijove longitudes and spacecraft orientations. The science planning process starts with the JSOC Science Planner creating an Activity Period (AP) for the duration of the planned sequence by referring to the Juno Mission Plan. An Engineering Activity Plan (EAP) containing the list of DSN passes, engineering activities and KOZs is produced by the Mission Planning and Sequencing Team (MPST). A power profile file which lists the power available for use by the payload is created by the Spacecraft Team. The JSOC import functionality is used to import these files and populate fields in the AP. The JSOC science planner also creates epochs for referencing instrument activity start and end times. Figure 7 shows data flow between entities involved in the science planning process.

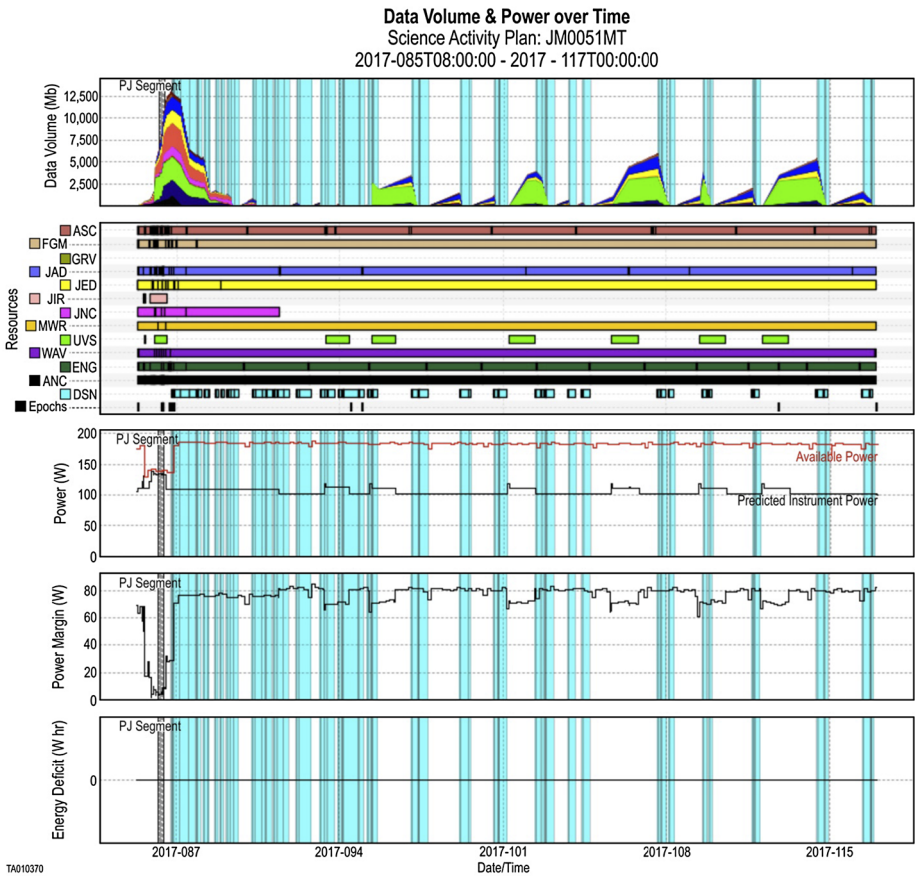


Fig. 10 Summary charts from the validation page of the SAP for the JM0051 sequence containing perijove 5. The *first panel* shows a stacked graph of data volume over time in the framed data partitions with each color representing an instrument. *Vertical turquoise bands* indicate DSN passes where the data get downlinked. The *second panel* shows instrument activities. The *third panel* shows available power and predicted power used by the payload. The next two panels show power margin and the energy deficit, which in this case is zero for the entire duration since the power margin is positive

SAPs are typically instantiated by copying a template SAP or an earlier SAP into the activity period for the sequence under development. The available data volume is allocated to the instruments by the Science Planning Working Group and recorded by the JSOC Science Planner in the SAP, along with other agreements. Instrument teams work on adding and updating their activities to meet science objectives and be within the resource constraints. They may copy the Draft SAP and create Trial SAPs to evaluate and validate different scenarios. They may also copy IAs from different SAPs into the target SAP.

When IA updates are complete, JSOC validates the SAP to determine if the predicted resources are within the available limits. If problems are found during validation, JSOC science planners work with the SPWG and the IOTs to determine necessary changes to be implemented. When validation is successful, the SAP status is first promoted to Pending for further power modeling by the SCT and after the sequence kickoff meeting, promoted to Approved status and locked. The SAP can be exported in multiple formats. Instrument teams

use the ASCII export of the SAP to produce their command sequences using automated or manual means in the form of Spacecraft Activity Sequence Files (SASF). Instrument teams send these directly to the MPST for validation, verification and uplink.

3.5 Data Management Process

3.5.1 Instrument Data Delivery

Telemetry from Juno is downlinked by the DSN stations and delivered to the IOTs by the Juno Ground Data System (GDS) at JPL after reconstruction. IOTs extract the data and convert from engineering units to dimensional values in the form of PDS compliant level-2 data files, associated label files and structure files if any. These files are uploaded by the IOTs to the JSOC staging server using SFTP either individually or as a compressed zip archive. Data management applications on the JSOC server automatically pick up the files, decompress if necessary, and perform validation to determine if the files comply with JSOC rules and then perform a second validation using tools supplied by PDS to determine compliance.

The results of both validations are communicated to the instrument teams and JSOC data analysts immediately by email. If the files are compliant, they get ingested into the file system along with their catalog records. If any files are not compliant, the email messages specify the errors and those files are held in a temporary location for inspection. JSOC data analysts work with the IOTs to resolve the errors and warnings. The destination directory of the files is determined using rules developed by JSOC analysts in consultation with the IOTs. These rules use data filenames and keywords in the label file to determine the destination and are entered into a configuration file for each instrument which gets read during ingestion. As instrument teams process and enhance their data, level-3 and higher-level data products are produced, and similarly delivered to JSOC.

These files can be accessed using a JSOC SFTP read only directory or by using the JSOC website. The JSOC data management module provides filters to search for files by instrument, type, date range, etc. and a way to download individual files or a zip archive containing multiple selected files.

3.5.2 Data Archiving

The final step is the delivery of the archive volumes to the PDS to archive in the public domain. JSOC works with the Juno Data Archive Working Group (DAWG) comprised of a chair, IOTs, JSOC, and PDS representatives to create a schedule for delivery of data volumes to PDS.

The JSOC software includes a module that prepares archive data sets. In addition to the data and label files, IOTs also deliver supplementary files to build the archive set. JSOC data analysts select the products to be included in each archive data set in consultation with the IOT by using the search functions and then tagging the files. Once the full set of files is selected, functionality also exists to create an index file for the archive volume and the associated checksums. After receiving authorization from the instrument team lead and the PI, a delivery package is created and transmitted it to the appropriate PDS node.

3.6 Science Team Support Functions

The JSOC data system queries NAIF's servers for generic and Juno specific SPICE kernels twice a day to copy all new and updated kernels to the JSOC system. JSOC users can use

either an interactive webpage or a command line web-service function to generate a list of kernels and a metakernel. The JSOC Meetings and Documents module provides a central easy to use repository for the Juno team to share operations, planning and science documents as well as science team meeting presentations and public outreach material with appropriate export control permissions.

4 Summary

The Juno mission fills a long-recognized gap in NASA's plans for exploring Jupiter, as the first mission devoted to studying the interior of the solar system's largest planet. Juno's science objectives span Jupiter's origin and interior through its atmosphere all the way out to its luminous aurora and polar magnetosphere. As Juno had a successful launch, cruise, and Jupiter orbit insertion, we expect the data set it provides to drive our understanding of Jupiter for the foreseeable future.

Acknowledgements The Juno mission would not have been possible without the incredible dedication, commitment, and experience of the many hundreds of people who have worked on Juno. To call out a few by name would feel like a disservice to those not mentioned. They each have our incredible gratitude and appreciation for their efforts. In addition, we benefitted tremendously from the strong support from each of our partner organizations. Funding for the Juno mission was provided by NASA.

References

- A. Adriani, A. Coradini, G. Filacchione, J.I. Lunine, A. Bini, C. Pasqui, L. Calamai, F. Colosimo, B.M. Dinelli, D. Grassi, G. Magni, M.L. Moriconi, R. Orosei, JIRAM, the image spectrometer in the near-infrared on board the Juno mission to Jupiter. *Astrobiology* **8**, 613–622 (2008)
- A. Adriani, G. Filacchione, T. Di Iorio et al., JIRAM, the Jovian Infrared Auroral Mapper. *Space Sci. Rev.* (2017). doi:[10.1007/s11214-014-0094-y](https://doi.org/10.1007/s11214-014-0094-y)
- Y. Alibert, C. Mordasini, W. Benz, C. Winisdoerffer, Models of giant planet formation with migration and disc evolution. *Astron. Astrophys.* **434**, 343–353 (2005)
- S.W. Asmar, S.J. Bolton, D.R. Buccino et al., The Juno gravity science instrument. *Space Sci. Rev.* (2017). doi:[10.1007/s11214-017-0428-7](https://doi.org/10.1007/s11214-017-0428-7)
- S.K. Atreya, M.H. Wong, T.C. Owen, P.R. Mahaffy, H.B. Niemann, I. de Pater, P. Drossart, T. Encrenaz, A comparison of the atmospheres of Jupiter and Saturn: deep atmospheric composition, cloud structure, vertical mixing, and origin. *Planet. Space Sci.* **47**, 1243–1262 (1999)
- F. Bagenal, A. Adriani, F. Allegrini et al., Magnetospheric science objectives of the Juno mission. *Space Sci. Rev.* (2017). doi:[10.1007/s11214-014-0036-8](https://doi.org/10.1007/s11214-014-0036-8)
- I. Baraffe, G. Chabrier, T. Barman, Structure and evolution of super-Earth to super-Jupiter exoplanets. I. Heavy element enrichment in the interior. *Astron. Astrophys.* **482**, 315–332 (2008)
- H.N. Becker, J.W. Alexander, A. Adriani et al., The Juno Radiation Monitoring (RM) investigation. *Space Sci. Rev.* (2017). doi:[10.1007/s11214-017-0345-9](https://doi.org/10.1007/s11214-017-0345-9)
- D.E. Bernard, R.D. Abelson, J.R. Johannesen et al., Europa planetary protection for Juno Jupiter orbiter. *Adv. Space Res.* **52**, 547–568 (2013). doi:[10.1016/j.asr.2013.03.015](https://doi.org/10.1016/j.asr.2013.03.015)
- B. Bonfond, D. Grodent, J.-C. Gérard, T. Stallard, J.T. Clarke, M. Yoneda, A. Radioti, J. Gustin, Auroral evidence of Io's control over the magnetosphere of Jupiter. *Geophys. Res. Lett.* **39**, 1105 (2012)
- A.P. Boss, Evolution of the solar nebula. IV. Giant gaseous protoplanet formation. *Astrophys. J.* **503**, 923–937 (1998)
- A.P. Boss, Formation of gas and ice giant planets. *Earth Planet. Sci. Lett.* **202**, 513–523 (2002). doi:[10.1016/S0012-821X\(02\)00808-7](https://doi.org/10.1016/S0012-821X(02)00808-7)
- F.H. Busse, A simple model of convection in the Jovian atmosphere. *Icarus* **29**, 255–260 (1976)
- J.E. Chambers, G.W. Wetherill, Making the terrestrial planets: N-body integrations of planetary embryos in three dimensions. *Icarus* **136**, 304–312 (1998)
- J.E.P. Connerney, M.H. Acuna, N.F. Ness, Modeling the Jovian current sheet and inner magnetosphere. *J. Geophys. Res.* **86**, 8370–8384 (1981)

- J.E.P. Connerney, M.H. Açuna, N.F. Ness, T. Satoh, New models of Jupiter's magnetic field constrained by the Io Flux Tube footprint. *J. Geophys. Res.* **103**, 11929–11939 (1998)
- J.E.P. Connerney, M. Benn, J.B. Bjarno et al., The Juno magnetic field investigation. *Space Sci. Rev.* (2017). doi:[10.1007/s11214-017-0334-z](https://doi.org/10.1007/s11214-017-0334-z)
- B.J. Conrath, D. Gautier, Saturn helium abundance: a reanalysis of Voyager measurements. *Icarus* **144**, 124–134 (2000)
- R.W. Ebert, F. Bagenal, D. McComas, C. Fowler, A survey of solar wind conditions at 5 AU: a tool for interpreting solar wind-magnetosphere interactions at Jupiter. *Front. Astron. Space Sci.* **1**, 4 (2014)
- J.J. Fortney, W.B. Hubbard, Phase separation in giant planets: inhomogeneous evolution of Saturn. *Icarus* **164**, 228–243 (2003)
- J.J. Fortney, W.B. Hubbard, Effect of helium phase separation on the evolution of extrasolar giant planets. *Astrophys. J.* **608**, 1039–1049 (2004)
- J.J. Fortney, M. Ikoma, N. Nettleman, T. Guillot, M.S. Marley, Self-consistent model atmospheres and the cooling of the solar system's giant planets. *Astrophys. J.* **729**, 32 (2011), 14pp.
- M. French, A. Becker, W. Lorenzen, N. Nettelmann, M. Bethkenhagen, J. Wicht, R. Redmer, Ab initio simulations for material properties along the Jupiter adiabat. *Astrophys. J. Suppl.* **202**, 5 (2012). doi:[10.1088/0067-0049/202/1/5](https://doi.org/10.1088/0067-0049/202/1/5)
- D. Gautier, F. Hersant, O. Mousis, J.I. Lunine, Enrichments in volatiles in Jupiter: a new interpretation of the Galileo measurements. *Astrophys. J. Lett.* **550**, L227–L230 (2001) (Erratum **559**, L183)
- P.J. Gierasch, A.P. Ingersoll, D. Banfield, S.P. Ewald, P. Helfenstein, A. Simon-Miller, A. Vasavada, H.H. Breneman, D.A. Senske (Galileo Imaging Team), Observation of moist convection in Jupiter's atmosphere. *Nature* **403**, 628–630 (2000)
- G.R. Gladstone, S.C. Persyn, J.S. Eterno et al., The ultraviolet spectrograph on NASA's Juno mission. *Space Sci. Rev.* (2014). doi:[10.1007/s11214-014-0040-z](https://doi.org/10.1007/s11214-014-0040-z)
- R.S. Grammier, A look inside the Juno mission to Jupiter. IEEE Aerospace Conference, paper #1582 (2009)
- D. Grodent, J.T. Clarke, J. Kim, J.H. Waite Jr., S.W.H. Cowley, Jupiter's main auroral oval observed with HST-STIS. *J. Geophys. Res.* **108**, 1389 (2003)
- S.M. Guertin, G.R. Allen, D.J. Sheldon, *Programmatic Impact of SDRAM SEFI*, 16–20 July 2012, IEEE Radiation Effects Data Workshop (2012). doi:[10.1109/REDW.2012.6353722](https://doi.org/10.1109/REDW.2012.6353722)
- T. Guillot, A comparison of the interiors of Jupiter and Saturn. *Planet. Space Sci.* **47**, 1175–1182 (1999)
- T. Guillot, The interiors of giant planets: models and outstanding questions. *Annu. Rev. Earth Planet. Sci.* **33**, 493–530 (2005)
- T. Guillot, D. Gautier, W.B. Hubbard, New constraints on the composition of Jupiter from Galileo measurements and interior models. *Icarus* **130**, 534–539 (1997)
- T. Guillot, D.J. Stevenson, W.B. Hubbard, D. Saumon, The interior of Jupiter, in *Jupiter*, ed. by F. Bagenal et al. (Cambridge University Press, Cambridge, 2004), pp. 35–57, Chap. 3
- C.J. Hansen, M.A. Caplinger, A. Ingersoll et al., JunoCam: Juno's outreach camera. *Space Sci. Rev.* (2017). doi:[10.1007/s11214-014-0079-x](https://doi.org/10.1007/s11214-014-0079-x)
- P. Helled, M. Podolak, A. Kovetz, Planetesimal capture in the disk instability model. *Icarus* **185**, 64–71 (2006)
- F. Hersant, D. Gautier, F. Huré, A two-dimensional model for the primordial nebula constrained by D/H measurements in the Solar System: implications for the formation of giant planets. *Astrophys. J.* **554**, 391–407 (2001)
- F. Hersant, D. Gautier, J.I. Lunine, Enrichment in volatiles in the giant planets of the Solar System. *Planet. Space Sci.* **52**, 623–641 (2004)
- W.B. Hubbard, Thermal structure of Jupiter. *Astrophys. J.* **152**, 745–754 (1968)
- W.B. Hubbard, The Jovian surface condition and cooling rate. *Icarus* **30**, 305–310 (1977)
- W.B. Hubbard, Gravitational signature of Jupiter's deep zonal flows. *Icarus* **137**, 357–359 (1999)
- A.P. Ingersoll, D. Pollard, Motion in the interiors and atmospheres of Jupiter and Saturn—scale analysis, anelastic equations, barotropic stability criterion. *Icarus* **52**, 62–80 (1982)
- M.E. Janssen, J.E. Oswald, S.T. Brown, S. Gulkis, S.M. Levin, S.J. Bolton, M.D. Allison, S.K. Atreya, D. Gautier, A.P. Ingersoll, J.I. Lunine, G.S. Orton, T.C. Owen, P.G. Steffes, V. Adumitroaie, A. Belloti, L.A. Jewell, C. Li, L. Li, F.A. Oyafuso, D. Santos-Costa, E. Sarkissian, R. Williamson, J.K. Arballo, A. Kityakara, A. Ulloa-Severino, J.C. Chen, F.W. Maiwald, A.S. Sahakian, P.J. Pingree, K.A. Lee, A.S. Mazer, R. Redick, R.E. Hodges, R.C. Hughes, G. Bedrosian, D.E. Dawson, W.A. Hatch, D.S. Russell, N.F. Chamberlain, M.S. Zawadzki, B. Khayatian, B.R. Franklin, H.A. Conley, J.G. Kempenaar, M.S. Loo, E.T. Sunada, V. Vorperion, C.C. Wang, MWR microwave radiometer for the Juno mission to Jupiter. *Space Sci. Rev.* (2017). doi:[10.1007/s11214-017-0349-5](https://doi.org/10.1007/s11214-017-0349-5)
- S.P. Joy, M.G. Kivelson, R.J. Walker, K.K. Khurana, C.T. Russell, T. Ogino, Probabilistic models of the Jovian magnetopause and bow shock locations. *J. Geophys. Res.* **107**, A101309 (2002). doi:[10.1029/2001JA009146](https://doi.org/10.1029/2001JA009146)

- S. Kayali, W. McAlpine, H. Becker, L. Scheick, in *Juno Radiation Design and Implementation*, IEEE Aerospace Conf., 3–10 March 2012 (2012), 3–10. doi:[10.1109/AERO.2012.6187013](https://doi.org/10.1109/AERO.2012.6187013)
- W.S. Kurth, G.B. Hospodarsky, D.L. Kirchner et al., The Juno waves investigation, *Space Sci. Rev.* (2017). doi:[10.1007/s11214-017-0396-y](https://doi.org/10.1007/s11214-017-0396-y)
- J. Leconte, G. Chabrier, A new vision of giant planet interiors: impact of double diffusive convection. *Astron. Astrophys.* **540**, A20 (2012), 13 pp
- J. Lewis, Juno spacecraft operations lessons learned for early cruise mission phases. IEEE Aerospace Conference (2014)
- G.F. Lindal, G.E. Wood, G.S. Levy, J.D. Anderson, D.N. Sweetnam, H.B. Hotz, B.J. Buckles, D.P. Holmes, P.E. Doms, V.R. Eshleman, G.L. Tyler, T.A. Croft, The atmosphere of Jupiter—an analysis of the Voyager radio occultation measurements. *J. Geophys. Res.* **86**, 8721–8727 (1981)
- J.J. Lissauer, Planet formation. *Annu. Rev. Astron. Astrophys.* **31**, 129–174 (1993)
- K. Lodders, Jupiter formed with more tar than ice. *Astrophys. J.* **611**, 587–597 (2004)
- F. Low, Infrared observations of Venus, Jupiter and Saturn at $\lambda 20\mu$. *Astron. J.* **71**, 391 (1966)
- M. Lozovsky, R. Helled, E.D. Rosenberg, P. Bodenheimer, Jupiter's formation and its primordial internal structure. *Astrophys. J.* **836**, 1–31 (2017). doi:[10.3847/1538-4357/836/2/227](https://doi.org/10.3847/1538-4357/836/2/227)
- J.I. Lunine, D.M. Hunten, Moist convection and the abundance of water in the troposphere of Jupiter. *Icarus* **69**, 566–570 (1987)
- B.H. Mauk, D.K. Haggerty, S.E. Jaskulek et al., The Jupiter energetic particle detector instrument (JEDI) investigation for the Juno mission. *Space Sci. Rev.* (2013). doi:[10.1007/s11214-013-0025-3](https://doi.org/10.1007/s11214-013-0025-3)
- L. Mayer, T. Quinn, J. Wadsley, J. Stadel, Formation of giant planets by fragmentation of protoplanetary disks. *Science* **298**, 1756–1759 (2002)
- D.J. McComas, N. Alexander, F. Allegrini et al., The Jovian Auroral Distributions Experiment (JADE) on the Juno mission to Jupiter. *Space Sci. Rev.* (2013). doi:[10.1007/s11214-013-9990-9](https://doi.org/10.1007/s11214-013-9990-9)
- B. Militzer, W.B. Hubbard, J. Vorberger, I. Tamblyn, S.A. Bonev, *Astrophys. J.* **688**, L45 (2008)
- H. Mizuno, Formation of the giant planets. *Prog. Theor. Phys.* **64**, 544–557 (1980)
- O. Mousis, J.I. Lunine, N. Madhusudhan, T.V. Johnson, Nebular water depletion as the cause of Jupiter's low oxygen abundance. *Astrophys. J. Lett.* **751**, L7 (2012). doi:[10.1088/2041-8205/751/1/L7](https://doi.org/10.1088/2041-8205/751/1/L7)
- N. Nettelmann, B. Holst, A. Kietzmann, M. French, R. Redmer, Ab initio equation of state data for hydrogen, helium, and water and the internal structure of Jupiter. *Astrophys. J.* **683**, 1217–1228 (2008)
- R. Nybakken, The Juno mission to Jupiter—a pre-launch update. IEEE Aerospace Conference paper #1179 (2011)
- R. Nybakken, The Juno mission to Jupiter—launch campaign and early cruise report. IEEE Aerospace Conference (2012)
- T. Owen, Th. Encrenaz, Element abundances and isotopic ratios in the giant planets and Titan. *Space Sci. Rev.* **106**, 121–138 (2003)
- T. Owen, P. Mahaffy, H.B. Niemann, S.K. Atreya, T.M. Donahue, A. Bar-Nun, I. de Pater, A low temperature origin for the planetesimals that formed Jupiter. *Nature* **402**, 269–270 (1999)
- J.B. Pollack, O. Hubickyj, P. Bodenheimer, J.J. Lissauer, M. Podolak, Y. Greenzweig, Formation of the giant planets by concurrent accretion of solids and gas. *Icarus* **124**, 62–85 (1996a)
- J.B. Pollack, O. Hubickyj, P. Bodenheimer, J.J. Lissauer, M. Podolak, Y. Greenzweig, A review of hydrogen, carbon, nitrogen, oxygen, sulphur, and chlorine stable isotope enrichment among gaseous molecules. *Icarus* **124**, 62–85 (1996b)
- D. Saumon, T. Guillot, Shock compression of deuterium and the interiors of Jupiter and Saturn. *Astrophys. J.* **609**, 1170–1180 (2004)
- D. Saumon, W.B. Hubbard, A. Burrows, T. Guillot, J.I. Lunine, G. Chabrier, A theory of extrasolar giant planets. *Astrophys. J.* **460**, 993–1018 (1996)
- A. Seiff, D.B. Kirk, T.C.D. Knight, R.E. Young, J.D. Mihalov, L.A. Young, F.S. Milos, G. Schubert, R.C. Blanchard, D. Atkinson, Thermal structure of Jupiter's atmosphere near the edge of a 5- μ m hot spot in the North equatorial belt. *J. Geophys. Res.* **103**, 22857–22890 (1998)
- A.P. Showman, T.E. Dowling, Nonlinear simulations of Jupiter's 5-micron hot spots. *Science* **289**, 1737–1740 (2000)
- S.K. Stephens, The Juno mission to Jupiter: lessons from cruise and plans for orbital operations and science return. IEEE Aerospace Conference, paper # 2150 (2015)
- D.J. Stevenson, Thermodynamics and phase separation of dense fully ionized hydrogen-helium fluid mixtures. *Phys. Rev. B* **12**, 3999–4007 (1975)
- D.J. Stevenson, Planetary magnetic fields: achievements and prospects. *Space Sci. Rev.* (2009). doi:[10.1007/s11214-009-9572-z](https://doi.org/10.1007/s11214-009-9572-z)
- D.J. Stevenson, E.E. Salpeter, The dynamics and helium distribution in hydrogen-helium planets. *Astrophys. J. Suppl. Ser.* **35**, 239–261 (1977)

- U. Von Zahn, D.M. Hunten, G. Lehmacher, Helium in Jupiter's atmosphere: results from the Galileo probe helium interferometer experiment. *J. Geophys. Res.* **103**, 22815–22829 (1998)
- H.F. Wilson, B. Militzer, Solubility of water ice in metallic hydrogen: consequences for core erosion in gas giant planets. *Astrophys. J.* **745**, 54 (2011)
- H.F. Wilson, B. Militzer, Rocky core solubility in Jupiter and giant exoplanets. *Phys. Rev. Lett.* **108**, 111101 (2012)
- M.H. Wong, P.R. Mahaffy, S.K. Atreya, H.B. Niemann, T.C. Owen, Updated Galileo probe mass spectrometer measurements of carbon, oxygen, nitrogen, and sulfur on Jupiter. *Icarus* **171**, 153–170 (2004)
- M.H. Wong, J.I. Lunine, S.K. Atreya, T. Johnson, P.R. Mahaffy, T.C. Owen, T. Encrenaz, Oxygen and other volatiles in the giant planets and their satellites. *Rev. Mineral. Geochem.* **68**, 219–246 (2008)
- G. Wuchterl, T. Guillot, J.J. Lissauer, Giant planet formation, in *Protostars and Planets IV*, ed. by V. Mannings, A.P. Boss, S.S. Russell (University of Arizona Press, Tucson, 2000), pp. 1081–1109